TelePulse: Enhancing the Teleoperation Experience through Biomechanical Simulation-Based Electrical Muscle Stimulation in Virtual Reality

Seokhyun Hwang*
Information School
University of Washington
Seattle, Washington, USA
Human-Centered Intelligent Systems Lab
Gwangju Institute of Science and Technology
Gwangju, Republic of Korea
seokhyun@uw.edu

Seongjun Kang*
Human-Centered Intelligent Systems Lab
Gwangju Institute of Science and Technology
Gwangju, Republic of Korea
ksjryan0728@gm.gist.ac.kr

Jeongseok Oh*
Human-Centered Intelligent Systems Lab
Gwangju Institute of Science and Technology
Gwangju, Republic of Korea
jungseok17@gm.gist.ac.kr

Jeongju Park
Human-Centered Intelligent Systems Lab
Gwangju Institute of Science and Technology
Gwangju, Republic of Korea
jeongjupark@gm.gist.ac.kr

Semoo Shin
Human-Centered Intelligent Systems Lab
Gwangju Institute of Science and Technology, Gwangju, Republic of Korea
sms081700@gm.gist.ac.kr

Yiyue Luo
ECE
University of Washington
Seattle, Washington, USA
yiyueluo@uw.edu

Joseph DelPreto
Distributed Robotics Lab
Massachusetts Institute of Technology (MIT)
Cambridge, Massachusetts, USA
delpreto@csail.mit.edu

Sangbeom Lee
Artificial Intelligence Lab
Gwangju Institute of Science and Technology
Gwangju, Republic of Korea
saturnbeom@gm.gist.ac.kr

Kyoobin Lee
Artificial Intelligence Lab
Gwangju Institute of Science and Technology
Gwangju, Republic of Korea
kyoobinlee@gist.ac.kr

Wojciech Matusik
CSAIL
MIT
Cambridge, Massachusetts, USA
wojciech@csail.mit.edu

Daniela Rus
Distributed Robotics Lab
Massachusetts Institute of Technology
Cambridge, Massachusetts, USA
rus@csail.mit.edu

SeungJun Kim†
Human-Centered Intelligent Systems Lab
Gwangju Institute of Science and Technology
Gwangju, Republic of Korea
seungjun@gist.ac.kr

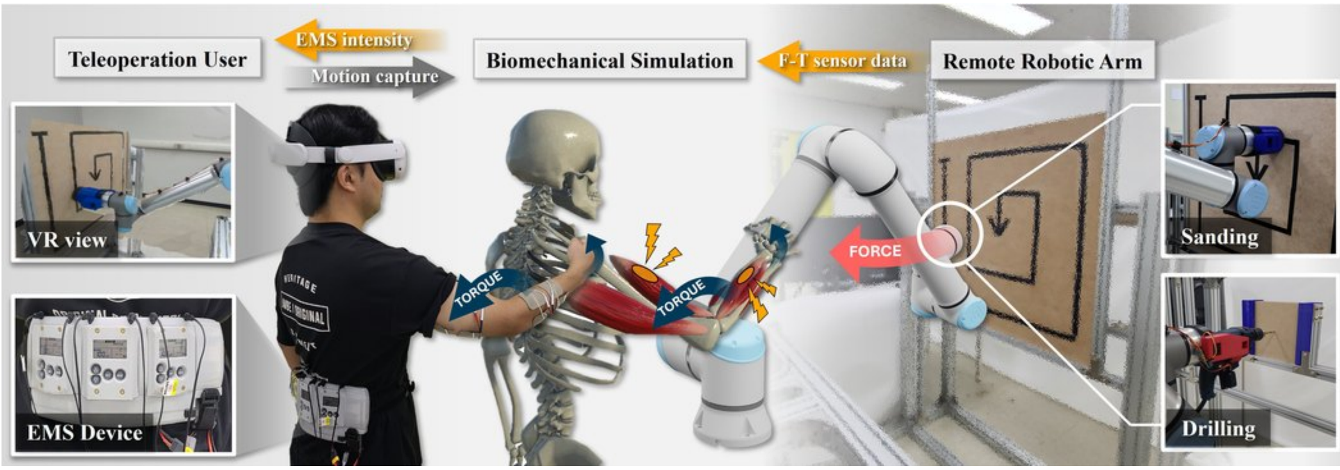

Figure 1: The conceptual graphical representation of the system that provides force feedback measured from the teleoperation workspace to the remote worker. The interaction force between the remote environment and the robot is transformed into EMS signals based on the user's real-time motion capture through biomechanical simulation and delivered to the user.

Abstract

This paper introduces TelePulse, a system integrating biomechanical simulation with electrical muscle stimulation (EMS) to provide precise haptic feedback for robot teleoperation tasks in virtual reality (VR). TelePulse has two components: a physical simulation part that calculates joint torques based on real-time force data from remote manipulators, and an electrical stimulation part that converts these torques into muscle stimulation. Two experiments were conducted to evaluate the system. The first experiment assessed the accuracy of EMS generated through biomechanical simulations by comparing it with electromyography (EMG) data during force-directed tasks, while the second experiment evaluated the impact of TelePulse on teleoperation performance during sanding and drilling tasks. The results suggest that TelePulse provided more accurate stimulation across all arm muscles, thereby enhancing task performance and user experience in the teleoperation environment. In this paper, we discuss the effect of TelePulse on teleoperation, its limitations, and areas for future improvement.

CCS Concepts

• **Human-centered computing → Haptic devices**; **Virtual reality**.

Keywords

Teleoperation; Virtual Reality; Haptic; Electrical Muscle Stimulation; Biomechanics; Simulation; Wearable Device

*These authors contributed equally to this work.
†Corresponding author.

CHI '25, Yokohama, Japan

ACM ISBN 979-8-4007-1394-1/25/04
https://doi.org/10.1145/3706598.3713767

ACM Reference Format:
Seokhyun Hwang, Seongjun Kang, Jeongseok Oh, Jeongju Park, Semoo Shin, Yiyue Luo, Joseph DelPreto, Sangbeom Lee, Kyoobin Lee, Wojciech Matusik, Daniela Rus, and SeungJun Kim. 2025. TelePulse: Enhancing the Teleoperation Experience through Biomechanical Simulation-Based Electrical Muscle Stimulation in Virtual Reality. In *CHI Conference on Human Factors in Computing Systems (CHI '25), April 26–May 01, 2025, Yokohama, Japan.* ACM, New York, NY, USA, 26 pages. https://doi.org/10.1145/3706598.3713767

1 Introduction

Teleoperation, the remote manual control of robots by human operators, is a technology applicable in various fields that require precise and safe human intervention. Despite significant advancements in autonomous robotic systems, teleoperation remains a primary method in complex and unpredictable environments such as surgery [84, 85, 108], space exploration [74, 104], disaster response [77, 90], and deep-sea exploration [11, 120]. Teleoperation leverages the operator's cognitive abilities to achieve high reliability in such challenging settings. However, it also imposes a considerable burden on the operator, who needs to interpret and execute tasks through a cumbersome interface. This challenge can be understood as the "gulf of execution and evaluation," [83] which represents the gap between the high-level objectives of the robotic system (e.g., surgical procedures or exploration) and the low-level input mechanisms available to the operator (e.g., joystick commands and monitor-based feedback) [113]. The difficulties posed by this gulf have been categorized into three issues: 1) confusion about which commands will achieve the given goal, 2) uncertainty about the impact of their commands on the system, and 3) potential physical dangers surrounding the robot system while it is executing commands [113]. Therefore, to address these challenges, current teleoperation research focuses on bridging the gulf between the operator and the remote system, aiming to improve user experience and task performance.

Recently, to address robot control challenges and enhance clarity in the execution and evaluation phases of human-robot interaction, researchers have been developing teleoperation systems that integrate virtual reality (VR) and haptic feedback technologies. The combination of VR and haptic feedback provides a immersive and realistic experience, enabling operators to receive tactile and force feedback in virtual environments, which enhances situational awareness and facilitates the execution of complex tasks [35, 45, 112]. Initially, haptic feedback in teleoperation was implemented using grounded mechanical devices [23, 95, 100], where robot manipulators were anchored to surfaces such as desks or the ground. These setups synchronized forces between the remote robot and its environment through identical [110] or scaled-down robotic models [2, 18]. Such systems have the advantage of providing users with sufficient and actual force feedback, but they are limited by their complexity, mobility, and high costs, thereby weakening the advantages of teleoperation, which allows tasks to be performed regardless of time and location. To overcome these limitations, recent research has focused on wearable haptic devices that offer greater mobility and cost-effectiveness. Wearable devices commonly utilize technologies such as vibration motors [9, 56], small actuators [1, 17], and electrotactile stimulation [88, 89] to provide tactile feedback. Wearable devices have addressed the previous limitations of grounded devices, enabling a more flexible and lightweight haptic teleoperation system; however, the small form factor of these devices confines the feedback to the skin's surface, limiting their ability to generate the realistic and actual force feedback required for delicate teleoperation tasks. In an effort to bridge the gap between grounded and wearable systems, some studies have explored exoskeleton-based wearable devices [8, 43]. While these exoskeletons can deliver actual force as haptic feedback, they present a technical trade-off: to provide actual and sufficient force, the inclusion of powerful actuators and batteries is necessary, which increases their weight, thereby reducing user mobility.

In light of these challenges, we propose a haptic feedback system, named ***TelePulse***, which combines biomechanical simulations with electrical muscle stimulation (EMS) to deliver realistic force feedback in a lightweight, wearable format suitable for teleoperation tasks. EMS induces muscle contractions through electrical stimulation, mimicking the natural process by which humans generate force. Distinct from traditional haptic devices, EMS does not rely on external actuators, enabling the simulation of large forces with relatively low power consumption and a compact size. However, EMS operates on individual muscles, requiring the stimulation of multiple muscles with varying intensities to accurately provide the forces resulting from interactions between the robot and the environment. In particular, determining the intensity, timing, and which muscles to stimulate with EMS requires real-time calculations based on the user's posture, forces from the remote robot, and the user's specific biomechanical characteristics, such as body length, joint movements, and weight. To address these challenges, TelePulse integrates biomechanical simulation, primarily used in the rehabilitation field, into a real-time VR environment, enabling it to calculate and deliver precise stimulation to the remote operator.

The TelePulse system proposed in this paper is divided into two main components: 1) the *physical simulation* component (**PhySim**) and 2) the *electrical stimulation* component (**EleStim**). The **PhySim** component is responsible for calculating the magnitude and direction of the forces that need to be provided to the user based on the kinematic data and force-torque (F-T) sensor data from the remote robotic manipulator. It then performs biomechanical simulations that consider user-specific characteristics such as posture, body length, joint movements, and weight, to compute the target torque for each joint in real-time. The **EleStim** component receives the target torque data from the **PhySim** component and converts it into EMS intensities that are personalized for the individual user. This enables the system to deliver the required force feedback as haptic sensations in real-time, providing a more immersive and accurate teleoperation experience, thereby improving task performance and user experience in teleoperation.

This paper discusses the development, implementation, and validation of the TelePulse system, and presents the results of two experiments conducted to assess its effectiveness. The first experiment focused on evaluating the accuracy of EMS intensities calculated through TelePulse's biomechanical simulations by comparing them with actual muscle activations measured via electromyography (EMG) sensors in an environment where forces were applied in various directions. The second experiment examined the system's ability to enhance task performance and user experience in actual teleoperation scenarios by conducting a live-user study. To provide a realistic working environment with various types of forces, we designed two different tasks: a sanding task with continuous force feedback and a drilling task with impulse force feedback. In these experimental environments, we compared TelePulse with two conditions: EMS without biomechanical simulation and an electrotactile condition commonly used in existing wearable haptic systems, allowing us to clearly identify the advantages of integrating biomechanical simulations within the TelePulse EMS system. The experiments demonstrate the potential of combining biomechanical simulations with EMS to improve the precision and effectiveness of haptic feedback in teleoperation environments, thereby enhancing task performance and overall user experience. This study addresses the following research questions:

- How accurately can TelePulse replicate natural muscle activations using biomechanical simulations and EMS during force-directed teleoperation tasks?
- Can TelePulse enhance user experience and task performance in teleoperation through biomechanical simulation based EMS?
- What are the limitations of using biomechanical simulations and EMS for haptic feedback in teleoperation, and how can these limitations be mitigated?

2 Background

2.1 Teleoperation Haptic System

Previous research on teleoperation haptic systems is broadly classified into grounded mechanical devices and body-attached devices. Grounded mechanical devices focus on delivering reliable force feedback for teleoperated tasks. Early work by Ueberle et al. [110] introduced a hyper-redundant haptic interface with 10 degrees of freedom (DOF) joints, demonstrating dexterity while maintaining precise force feedback for tool manipulation. This study highlights how grounded mechanical devices inherently excel in tasks requiring fine force rendering and singularity resolution. Subsequently, commercial haptic devices have emerged, offering scalable solutions for various applications. Ajoudani et al. [2] employed the *Novint Falcon* [40] to adapt robot impedance in real-time using position and stiffness references from the operator's arm. In both the medical and industrial domains, grounded mechanical devices have enabled the delivery of complex force feedback. Ze Cui et al. [18] used the *Phantom Premium* [28] for robotic surgery, achieving fine control over delicate tasks. González et al. [29] applied the *Phantom Omni* [27] for surface treatments, allowing precise force control in industrial environments. These studies highlight the capacity of grounded haptic systems to support tasks involving detailed and multi-dimensional force interactions. However, despite these advances, grounded mechanical devices face inherent limitations. Their large size and need for a stable base restrict operator mobility and workspace flexibility, confining users to predetermined workstations [23, 95, 100]. This constraint impacts the fundamental advantage of teleoperation—the ability to work independently of location—as operators remain confined to fixed setups.

To overcome these limitations, recent body-attached devices are primarily developed with an emphasis on portability and direct interaction with the user's arms. These systems successfully improve the mobility and wearability of haptic teleoperation systems by integrating various tactile feedback mechanisms, such as electrotactile feedback [88, 89, 103] and vibrotactile feedback [16, 26, 87, 118]. First, in studies using electrotactile feedback, Pamungkas et al. [88] utilized electrical stimulation in a teleoperated robotic arm to deliver tactile feedback, enhancing task precision in obstacle avoidance. Shahu et al. [103] further demonstrated its effectiveness in improving user performance beyond visual feedback alone. Second, vibrotactile feedback systems, Won et al. [118] developed a wireless vibration display device to replicate 3-DOF force feedback in a teleoperation system. Huang et al. [34] introduced *AeroHaptix*, a wearable system designed for UAV teleoperation that delivers directional vibrotactile feedback to enhance spatial awareness. Moreover, vibrotactile feedback has also been used for small-scale tactile perception. For example, Becker et al. [6] employed vibration signals linked to visuotactile sensors on a robot's end-effector, improving the perception of contact forces. Trinitatova and Tsetserukou [109] developed the *vDeltaGlove*, combining palm and fingertip feedback to deliver multimodal tactile sensations. These recent advancements illustrate significant progress in body-attached haptic devices, enhancing portability and providing more intuitive haptic feedback. Nevertheless, a limitation remains: the inability to replicate the magnitude and direction of actual forces experienced during interactions. By only providing surface-level haptic cues, these devices struggle to simulate large-scale force feedback applied to the entire arm.

In summary, while grounded mechanical devices offer actual force feedback and precise interaction with objects in remote environments, their large size and need for a stable base restrict the user's mobility and limit the range of motion during teleoperation. Conversely, body-attached devices enhance portability and allow for greater freedom of movement. However, these devices face challenges in replicating large-scale forces or actual torque feedback, limiting their ability to provide immersive haptic sensations. This technical trade-off between the precision of grounded devices and the mobility of body-attached systems is a major challenge in current research for designing effective teleoperation.

2.2 EMS Haptic System

EMS technology generates signals that stimulate muscle contractions by placing electrode pads near specific muscles, mimicking bioelectrical signals. This technique has been extensively studied in HCI research for its capability to deliver haptic feedback in virtual environments using small and lightweight devices without using external actuators [21, 42, 51, 54, 68, 70, 71, 111]. EMS offers the advantage of simulating realistic tactile feedback without the need for bulky physical devices. For example, in VR applications where users interact with heavy objects or encounter resistance, EMS can successfully stimulate the muscles responsible for counteracting these forces, simulating the sensation of lifting or pushing. Studies have shown that EMS can effectively simulate the sensation of interacting with virtual objects like walls, heavy boxes, or sliders, allowing users to feel the weight and resistance of objects [39, 51, 70, 71], and can also replicate physical impacts, such as collisions, by combining muscle stimulation with tactile cues [39, 68]. This feedback can be adjusted to ensure consistent perception of virtual elements, enabling users to experience force or impact feedback with greater immersion.

Although EMS has demonstrated its potential to deliver actual force with low power consumption and lightweight form without the need for external actuators, its application in teleoperation scenarios remains underexplored. The TelePulse system addresses these challenges by optimizing the location and intensity of muscle stimulation in real-time, considering the complex muscle and joint structures of the user's arm. Using biomechanical algorithms, the system simulates external forces and their interaction with the user's joints, providing realistic force feedback in teleoperation.

2.3 Biomechanical Simulation

Biomechanical simulations have been extensively applied in rehabilitation, especially for evaluating upper-limb functionality and assisting in the design of robotic assistive devices [4, 19, 30, 82, 101]. For example, in a study by Ayodele et al. [4], biomechanical simulations were used to simulate the interaction between a human arm and a rehabilitation robot, employing a dynamic arm model with 11 DOF. Similarly, Saputra et al. [101] developed a real-time control system for musculoskeletal models of the upper limb, demonstrating the efficacy of using biomechanical simulations in controlling wearable exoskeletons and robotic systems for arm rehabilitation.

Furthermore, these upper-limb biomechanical simulations have been integrated with VR environments, proving effective in improving motor recovery through immersive and motivational exercise experiences [7, 14]. Powell et al. [93, 94] integrated biomechanical simulation with a VR environment to accurately predict shoulder joint angles and forces during VR rehabilitation exercises, improving remote rehabilitation by providing therapists with real-time data on patient movements. Guo et al. [31] proposed a system for upper-limb force tracking within a digital twin VR environment using biomechanical simulations, offering dynamic, immersive scenarios tailored to the user's progress and improving exercise recovery through personalized feedback. These studies on the integration of biomechanical simulation and VR systems demonstrated that the motion of the real upper limb drove the virtual upper limb in real-time, dynamically measuring force and ensuring accurate muscle force analysis while enabling a non-invasive method.

Recently, extending beyond the application of biomechanical simulation in VR rehabilitation, several studies have been conducted to utilize it for providing realistic haptic sensations. Notably, research by Hwang et al. applied biomechanical simulations to lower-limb VR interactions, refining the realism of haptic feedback forces [39]. Their system, *ErgoPulse*, integrated biomechanical models to compute joint torques, converting them into EMS parameters designed to simulate forces such as water currents or the impact of kicking a soccer ball. The system ensured consistent force delivery that matched the user's biomechanical capabilities, reducing discrepancies in perceived force and enhancing overall task realism. Previous researches applying biomechanical simulations in VR has shown that these simulations can effectively replicate the kinematic properties of real users within a virtual space. In this study, we expanded on this approach by utilizing the biomechanical simulation to facilitate real-time interactions between a user's virtual twin in the virtual space and a robotic actuator in the real world, which possesses differing spatial and kinematic properties. In particular, these studies utilized *OpenSim* [19], an open-source biomechanics simulator, for biomechanical simulation, which is widely used to model upper-limb musculoskeletal structures, assess motor functions, and develop rehabilitation strategies. This enables a more immersive and realistic haptic experience by simulating arm motion and joint forces, utilizing the *OpenSim* platform to provide accurate feedback for teleoperation tasks. Therefore, to perform the biomechanical simulation for the TelePulse system proposed in this study, we utilized the *OpenSim* dynamic upper arm model.

3 Implementation

3.1 System Overview

The overall structure of the TelePulse system builds upon the structure of *ErgoPulse* by Hwang et al. [39]. While *ErgoPulse* focused on the forces acting on a virtual avatar synchronized with the real user, TelePulse accounts for interactions with a real-world robotic manipulator. Consequently, an interface for additional interactions between the user and the environment has been incorporated, as shown on the left side of Fig. 2. The teleoperation interface between the user and the environment is facilitated by a controller and a VR head-mounted display (HMD), as depicted on the left side of Fig. 2. Initially, the user sets the tool center point of the manipulator using the controller. The joint coordinates required for the manipulator to reach this target position are then calculated through inverse kinematics and communicated to the robot via TCP protocol. Simultaneously, the workspace, including the manipulator, is converted into a point cloud using the *Intel RealSense D435i*, and this data is presented to the user in VR through the *Unity engine*.

The proposed EMS haptic system consists of two key components: 1) the **PhySim** component and 2) the **EleStim** component. The **PhySim** component begins by acquiring upper body motion capture data from the *Meta Quest 3 Movement Software Development Kit* [75]. This motion capture is achieved through inside-out body tracking, using video data from the *Meta Quest 3* VR headset's external cameras—a pair of 4 Mpx RGB cameras and four 400 × 400 px IR cameras. The positional data for each joint, obtained through motion capture, is converted into joint coordinates using inverse kinematics. Using these coordinates, the system performs two separate inverse dynamics calculations. The first model (**Model 1** in Fig. 2) computes joint torques without incorporating external forces, while the second model (**Model 2** in Fig. 2) includes these external forces in its calculations. The difference between the joint torques derived from the two models indicates the torque magnitude that the EMS system must replicate.

To apply external forces in the simulation, we implemented two features—coordinate transformations and force scaling—tailored for teleoperation scenarios. First, in teleoperation, the coordinate frames of the forces and torques measured from the robotic manipulator differ from those of the user's hand and controller. To address this, we performed quaternion-based coordinate transformations to align the measured external forces with the biomechanical simulation. Detailed information about this process is provided in Section 3.4. Second, in teleoperation, the scale of force feedback resulting from interactions between the robotic manipulator and the environment may not align with the force scale achievable by the user using their own arm. For instance, teleoperation scenarios might include tasks such as clearing heavy building debris in construction sites or rescue operations, where forces exceed human capabilities, or performing delicate procedures like microsurgery on tiny blood vessels, where forces are below human perception thresholds. To address this, the external forces were adjusted to match the user's preferences through relative scaling after the coordinate transformation. However, in the experiments conducted for this study, we limited the force to 30 N due to the manipulator's safety limits, which fall within the average force range humans can typically exert during tasks. Consequently, despite being informed about this feature, all participants chose not to use the relative scaling function.

Next, the **EleStim** component of TelePulse determines the EMS intensity to generate the required torque calculated by the **PhySim** component. The characteristics and intensity of the EMS stimulus depend on the user's muscle properties and the placement of electrodes [22, 91]. Therefore, EMS strength must be individualized for each muscle, and electrode placement must be accurately mapped using anatomical landmarks to avoid unintended muscle activation. To tailor the EMS intensity, we establish the torque-intensity relationship for each user's muscles, as detailed in Section 3.2. The EMS stimulus, determined by this relationship, is subsequently transmitted to the user's arm muscles via a remotely controlled EMS device, allowing the user to experience the forces resulting from interactions between the remote manipulator and the environment.

3.2 Personalization Process of EMS

This section introduces the personalization process for TelePulse. As mentioned earlier, achieving accurate biomechanical simulations and EMS requires a personalization process tailored to individual characteristics, such as height, weight, bone length, and musculoskeletal properties. This personalization process is divided into two main stages: 1) geometrical calibration of the biomechanical

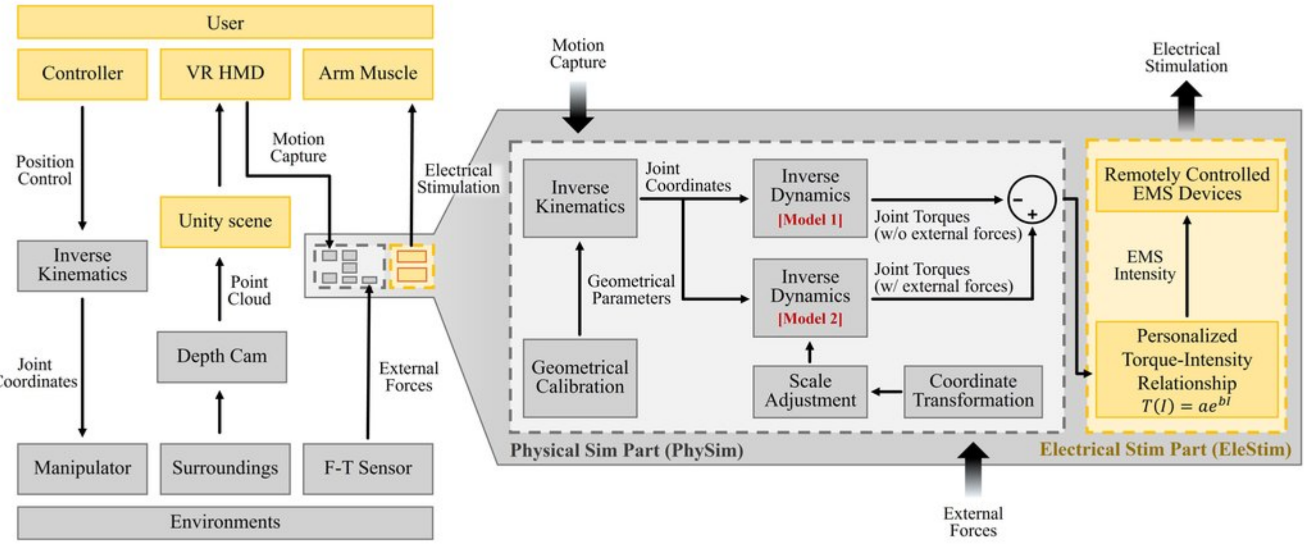

Figure 2: Overview of the TelePulse system. The diagram on the left illustrates the components of the user and environment, showing the data exchanged between them. The components of the biomechanical simulation are enlarged and highlighted on the right. The PhySim part on the right calculates joint torques, while the EleStim part adjusts EMS intensity for real-time muscle feedback.

simulation based on the user's body measurements, and 2) EMS calibration to determine the relationship between torque and stimulation intensity.

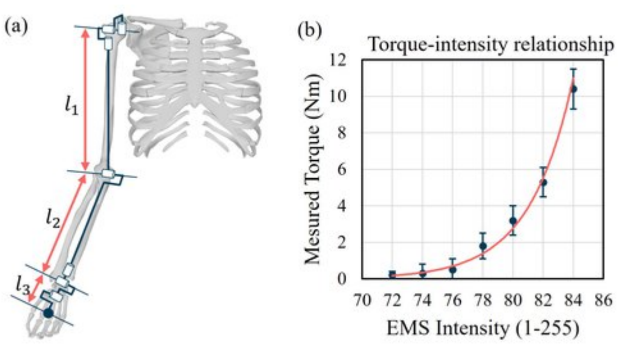

Figure 3: (a) Inter-joint distances of the participant for geometrical calibration, (b) EMS intensity to joint torque fitting.

First, during the geometrical calibration stage, we measured the distances between each joint for each participant, as illustrated in Fig. 3 (a). These measurements were used to perform a body retargeting process within the motion capture system, allowing for accurate simulation of the user's biomechanics. The total body mass of each participant was measured using a scale, and the weights of individual body segments (upper arm, lower arm, and hand) were estimated using the *Dempster biomechanical model* [20]. These data were then applied to the biomechanical simulation to create an individualized model for each user.

Second, since the relationship between EMS intensity and joint torque varies according to individual musculoskeletal characteristics, we calibrated each participant's muscles using a sigmoid-based torque-intensity graph fitting method used in rehabilitation and haptics fields [5, 12, 39, 57, 64, 65]. The EMS system used for haptic feedback applies stimuli within a range defined by the motor threshold (I_{MT}), the minimum stimulus intensity required to induce muscle contraction, and the pain threshold (I_{PT}), the maximum intensity that does not cause discomfort. The effective stimulation range lies within the acceleration region of the sigmoid-shaped torque-intensity curve [5, 12, 57, 65], where the relationship between torque (T) and stimulus intensity (I) is expressed as an exponential function (Fig. 3 (b)) with fitting parameters a and b, as shown in Eqn. 1:

$$T(I) = ae^{bI}(I_{MT} \leq I \leq I_{PT}) \tag{1}$$

In this experiment, we conducted simulations on six muscles: biceps brachii (Biceps), triceps brachii (Triceps), extensor carpi radialis longus (ECRL), extensor carpi ulnaris (ECU), flexor carpi radialis (FCR), and flexor carpi ulnaris (FCU) (Fig. 4). To measure I_{MT} and I_{PT} for each of these muscles, electrodes were attached to the participants, and the stimulus intensity was incrementally increased. Based on the participants' responses, the range of stimulation used in the experiment was determined (from minimum I_{MT} to maximum I_{PT}). Once the stimulation range was set, we used a custom calibration device to obtain the torque-intensity relationship curve for each of the participant's six muscles, as shown in Fig. 5. This device consists of load cells positioned to measure forces generated

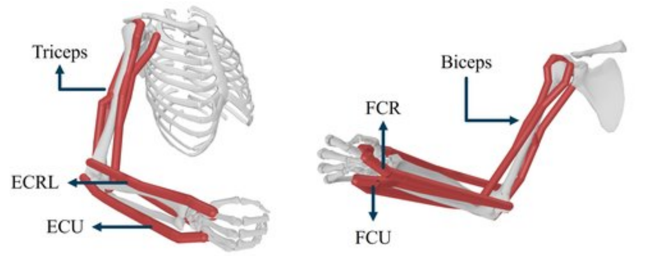

Figure 4: Enumerated muscles utilized in biomechanical simulation model. Six muscles are labeled: biceps brachii (Biceps), triceps brachii (Triceps), extensor carpi radialis longus (ECRL), extensor carpi ulnaris (ECU), flexor carpi radialis (FCR), and flexor carpi ulnaris (FCU).

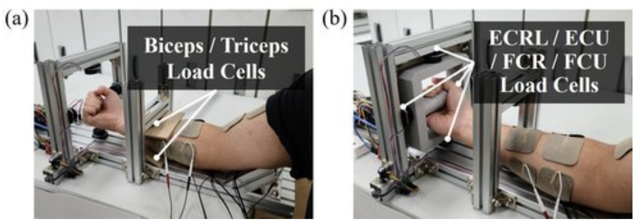

Figure 5: Calibration device for determining torque-intensity relationships. (a) Setup for biceps and triceps using load cells above and below the forearm. (b) Setup for ECRL, ECU, FCR, and FCU muscles using load cells in four directions with a handle.

by specific muscle groups. To ensure reliable calibration, we developed the device based on a load cell-based torque measurement device utilized in prior studies. Drawing on devices from earlier research that measured the torque-intensity graph for upper-body muscles [12, 57, 64, 67], we designed the device to firmly secure the user's muscles with bands and locking blocks, ensuring that torque generated by muscle contractions is not misinterpreted as unintended movements. In Fig. 5 (a), the calibration device is configured to measure the torque of the biceps and triceps, with load cells positioned above and below the forearm. For the remaining four muscles (ECRL, ECU, FCR, and FCU), Fig. 5 (b) illustrates a setup where the load cells are arranged to measure forces in the up, down, left, and right directions while the wrist is fixed. A handle is attached to the participant's hand to ensure stable positioning during the calibration process. To establish the torque-intensity relationship within this range, the interval between I_{MT} and I_{PT} was divided into seven segments, and the torque generated at each intensity level was measured three times using a load cell to ensure accuracy. The average torque values were then fitted to Eqn. 1, resulting in personalized torque-intensity curves for each of the six muscles, such as the one shown in Fig. 3 (b). This process allowed us to develop a personalized biomechanical model for each participant, ultimately enabling the calculation of joint torques and the corresponding EMS intensities required to replicate the forces experienced during teleoperation.

Through this comprehensive process, we created six distinct torque-intensity graphs for each participant. These relationships are then utilized by our system to determine the EMS intensity required to generate the appropriate joint torques in real-time, ensuring accurate haptic feedback during teleoperation.

3.3 Biomechanical Simulation Implementation

To perform biomechanical simulation tailored to individual users, our system constructs a personalized body model by incorporating details such as the length, weight, and relative position of each body segment, obtained through geometrical calibration. However, despite this process, the personalized model is still missing essential information for accurate simulation, such as the degrees of freedom, movement dynamics, range of motion, and the relative positions of joints and bones. Therefore, we utilized the *MoBL-ARMS Dynamic Upper Limb* model [73, 102] from the open-source software *OpenSim* [19] to gather detailed information on joint properties and the connections between body segments.

This customized body model is then integrated into our system, where it undergoes real-time inverse dynamics calculations using the *Nvidia PhysX* engine, a physics-based simulation platform within the *Unity* environment. By combining joint coordinate data obtained from real-time motion capture and inverse kinematics, the system considers gravitational forces and, when applicable (as in model 2 of Fig. 2), incorporates external forces measured by the F-T sensor attached to the *Universal Robots UR10e* robot. These components work together to calculate the torque applied to the user's joints in real-time, determining the specific torque that EMS needs to provide for each joint based on the current conditions.

3.4 Coordinate Transformation for Simulation

In teleoperation scenarios, the TelePulse system transmits the forces and torques experienced by the remote robotic manipulator to the user's arm. In contrast to other EMS systems that operate within a single coordinate frame, TelePulse requires a coordinate transformation process because the manipulator and the user exist in different coordinate systems.

We define three coordinate systems to facilitate this transformation: The **Manipulator Coordinate System** (C_m), attached to the robotic manipulator's end-effector where the force-torque sensor measurements $\mathbf{F}_m$ and $\mathbf{T}_m$ are obtained. The **World Coordinate System** (C_w), serving as the global reference frame in which both the manipulator and the user's arm are represented. The **User Coordinate System** (C_u), attached to the user's hand in the biomechanical simulation. To transform forces and torques from C_m to C_u, the relative rotation between these coordinate systems is computed directly using quaternions. Quaternions are selected for this transformation due to their computational efficiency and ability to avoid gimbal lock, which are particularly advantageous for real-time haptic feedback in teleoperation scenarios. Let $\mathbf{q}_{m \to w}$ and $\mathbf{q}_{u \to w}$ be the unit quaternions representing the orientations of the manipulator's end-effector and the user's hand in the world coordinate system C_w. The quaternion representing the rotation from the manipulator's coordinate system C_m to the user's coordinate system C_u is then obtained by:

$$\mathbf{q}_{m\to u} = \mathbf{q}_{m\to w} \otimes \mathbf{q}^*_{u\to w} \tag{2}$$

where $\otimes$ denotes quaternion multiplication and $\mathbf{q}^*$ is the conjugate of quaternion $\mathbf{q}$.

A unit quaternion $\mathbf{q} = [q_w, q_x, q_y, q_z]$ can be represented in terms of an axis-angle rotation, where $\mathbf{v} = [v_x, v_y, v_z]$ is the unit vector representing the axis of rotation and θ is the angle of rotation:

$$\mathbf{q} = [\cos(\theta/2), v_x \sin(\theta/2), v_y \sin(\theta/2), v_z \sin(\theta/2)] \tag{3}$$

Using the quaternion $\mathbf{q}_{m\to u}$, we transform the force $\mathbf{F}_m$ and torque $\mathbf{T}_m$ measured in C_m into C_u:

$$\mathbf{F}_u = |\mathbf{F}_m|(\mathbf{q}_{m\to u} \otimes \hat{\mathbf{F}}_m \otimes \mathbf{q}^*_{m\to u}) \tag{4}$$

$$\mathbf{T}_u = |\mathbf{T}_m|(\mathbf{q}_{m\to u} \otimes \hat{\mathbf{T}}_m \otimes \mathbf{q}^*_{m\to u}) \tag{5}$$

where $\hat{\mathbf{F}}_m$ and $\hat{\mathbf{T}}_m$ are the unit vectors of $\mathbf{F}_m$ and $\mathbf{T}_m$ respectively, treated as pure quaternions (quaternions with zero scalar part) during these operations. This approach allows for efficient rotation of the vectors while preserving their magnitudes, ensuring accurate transformation of both direction and magnitude of the force and torque from the manipulator's coordinate system to the user's coordinate system. These transformed forces and torques $\mathbf{F}_u$ and $\mathbf{T}_u$ are now expressed in the user's coordinate system and can be directly applied to the biomechanical model of the user's arm.

3.5 EMS Hardware Implementation

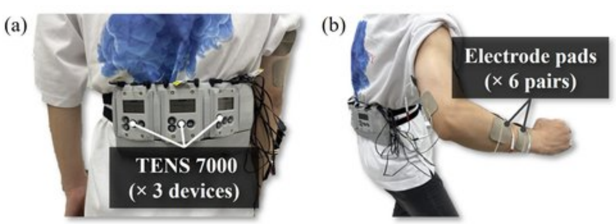

Figure 6: (a) The EMS device implemented in this study, worn around the participant's waist. (b) Electrodes attached to specific arm muscles for delivering remote EMS stimulation during the experiment.

In this study, we developed a hardware system to remotely deliver the computed EMS intensity to the operator, as shown in Fig. 6. The EMS signals were generated using the *TENS 7000* device, a medical-grade unit capable of delivering up to 100 mA of EMS. To ensure user safety, the signal generation module from the *TENS 7000* device was used without any modifications. The control and adjustment of EMS intensity were implemented using an *Arduino Nano 33 IoT microprocessor board* and an *AD5252 digital potentiometer*, based on methodologies from previous studies [68, 69, 91]. Electrodes were attached to six muscles, as shown in Fig. 6 (b). To control the EMS intensity, we incorporated a digital potentiometer, allowing adjustments in 255 discrete steps, as illustrated in Fig. 6 (a). This potentiometer is remotely controlled via Wi-Fi using WebSocket communication with a computer. To ensure system safety, the stimulation and control modules are electrically isolated. Additionally, a master switch, within easy reach of the participant, allows them to shut down all devices simultaneously at any time if they wish to stop. Based on previous research indicating that a signal frequency above 50 Hz is required to induce muscle contractions in participants [41, 55], we used a 100 Hz stimulation signal with this device. The system's overall delay was assessed using the *Unity Profiler*, with the total end-to-end delay measured at approximately 45 ms. This delay includes motion capture (≈ 15 ms), physical simulation (≈ 10 ms), Wi-Fi communication with the EMS device (≈ 5 ms), and muscle contraction latency (≈ 15 ms).

4 Experiment 1: Comparative Analysis of EMS Intensity and EMG Data in Force-Directed Tasks (E1)

The TelePulse system interprets the dynamics of a rigid body through biomechanical simulation, calculating the torque at each joint to provide force feedback to the arm via EMS. To assess the accuracy of the EMS intensities derived from biomechanical simulations, we compared the predicted muscle activation patterns with actual activations measured via EMG sensors. This comparison focused on how closely the simulated EMS-induced activations matched the muscle responses recorded during specific force-directed tasks in a teleoperation scenario.

4.1 Evaluation Setup

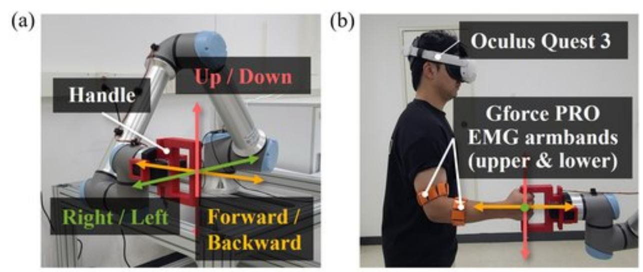

Figure 7: Experimental setup for the force-directed task. (a) The handle attached to the robotic arm's end tool, labeled with force directions: Up/Down, Forward/Backward, and Right/Left. (b) A participant wearing *Oculus Quest 3* for motion capture and *Gforce PRO EMG armbands* (upper & lower) for monitoring muscle activity.

To assess the correlation between the EMG data and the simulated EMS intensities, we designed a *force-directed task*. Participants were instructed to grasp the handle of the robotic arm's end tool, which was equipped with an F-T sensor, and perform a series of pushing tasks in six directions: up, down, left, right, forward, and backward (Fig. 7 (a)). The participants performed these tasks while standing on a platform positioned 30 cm from the end tool. Each participant wore two *OYmotion Gforce PRO* EMG armbands – one on the lower arm and one on the upper arm (Fig. 7 (b)) – to record real-time EMG data from six muscle groups: biceps, triceps, ECRL, ECU, FCR, and FCU. In addition, upper body motion capture data were collected using the *Oculus Quest 3* headset. The force and motion data collected during these tasks were subsequently used to estimate the EMS intensities required to induce the observed interaction forces.

To determine how accurately TelePulse's biomechanical simulation calculates EMS, we implemented two haptic systems and compared the EMS data calculated by each system to the actual EMG data from users. We compared the EMS intensities calculated through the biomechanical simulations method (labeled as **TelePulse**) and the method without biomechanical simulations, which simply adjusts the stimulus intensity proportionally to the force magnitude (labeled as **NonBioSim**), by assessing their similarity to the actual EMG data. This comparison specifically aimed to evaluate the effectiveness of biomechanical simulation in improving muscle activation accuracy across the six force directions. First, under the **TelePulse** condition, we used biomechanical simulations to calculate the EMS intensity required to generate the observed forces. The force applied by each participant, as recorded by the F-T sensor, along with the upper body motion capture data, was input into the simulations. Each participant completed the personalization process described in Section 3.2 prior to performing the EMS intensity calculations. Second, under the **NonBioSim** condition, we employed a conventional method without biomechanical simulation, where the EMS intensity was proportionally mapped to the maximum force of the robotic arm (45 N) and the participant's pain threshold (I_{PT}). The intensity was directly scaled to the F-T sensor readings, as done in previous upper limb haptic feedback studies [88, 89].

Procedure. Participants were equipped with *OYmotion Gforce PRO EMG armbands* on both the lower and upper arm of their dominant side, along with an *Oculus Quest 3* headset. They received a brief introduction on how to use the equipment before the experiment began. In the VR environment, participants could view the skeletal form of their arm as they grasped the robotic arm's end tool and performed pushing tasks in six directions: up, down, left, right, forward, and backward. For each direction, participants were instructed to push and hold the handle for 5 seconds after a 2-second preparation period, then release. This process was repeated three times per direction, totaling 18 trials (6 directions × 3 trials). Participants were instructed to maintain a stable posture, using only their arm muscles to exert force during the pushes. Before the experiment, participants were given approximately 2 minutes of practice time. Eight participants (age range: 22–25 years, M = 24.13, SD = 1.25, 5 males, 3 females) participated in the study, and all experiments were approved by the Institutional Review Board.

4.2 Results and Discussion

4.2.1 EMG Signal Processing. In E1, we aimed to assess the similarity between the EMS signals generated by TelePulse and *NonBioSim* in comparison to the actual EMG signals. To measure the similarity between EMS and EMG, we first analyzed the EMG signals, as shown in Fig. 8. Following the EMG signal analysis methods used in previous studies [3, 33, 78], we post-processed the EMG signals in three steps. Initially, we rectified the EMG signal by inverting the raw data with respect to the offset to calculate the rectified EMG signal (Fig. 8—Rectified EMG Signal). Next, we removed noise from the EMG signal using a low-pass filter (Fig. 8—Noise Filtered EMG Signal). We then performed linear envelope extraction after identifying the extrema from the noise-filtered signal, which smoothed the EMG signal into a refined curve (Fig. 8—Linear Enveloped EMG Signal). Through this process, we transformed the initially noisy EMG data into a corrected signal that could be directly compared with the EMS signal.

4.2.2 Similarity Between EMG and EMS. To calculate the similarity between the EMG and EMS signals, we first normalized both the EMG and EMS signals to align their scales. Additionally, we synchronized all signals along the time axis so that the EMS signals would rise simultaneously with the EMG as the muscles became activated. The processed TelePulse EMS signal, *NonBioSim* EMS signal, and EMG signal for each muscle are shown in Fig. 9. We measured the similarity between the EMG and EMS signals by applying the mean squared error (MSE) to assess the distance between them. For all conditions, the absolute values of skewness and kurtosis did not exceed 3.0 and 10.0, respectively, indicating that normality was satisfied [53]. We then applied the Student's t-test to examine the significance of the MSE values between TelePulse and *NonBioSim*. The detailed results of the statistical analyses and significance tests are presented in Table. 2 in Appendix A.

Precision of TelePulse Within the Muscles: The significance test on the EMS-EMG distance between TelePulse and *NonBioSim* revealed that the EMS signal from TelePulse had a significantly shorter distance to the EMG compared to *NonBioSim* ($p < .001^{***}$), demonstrating greater similarity to the activation of the actual user muscles. The results are shown in Fig. 10 (a). From these findings, we confirmed that TelePulse can provide stimulation with higher accuracy than *NonBioSim*. To further analyze this significance, we compared the EMS signals from TelePulse and *NonBioSim* with the EMG for each muscle, including the biceps, triceps, ECRL, ECU, FCR, and FCU. The results showed that TelePulse generated EMS signals closer to the EMG across all arm muscles, confirming that it can deliver muscle stimulation more closely aligned with real muscle activations.

Precision of TelePulse for Rendering Force Directions: The significance test indicated that, overall, TelePulse generated EMS signals that exhibited a smaller distance to the EMG signals produced when the user applied force in all six directions, compared to *NonBioSim* ($p < .001^{***}$). The results are shown in Fig. 10 (b). The results revealed that TelePulse produced EMS signals closer to the EMG signal patterns across all directions, suggesting that incorporating biomechanical simulation for precise muscle activation calculation brings superior results in rendering virtual force on the participant's arm in all six spatial directions.

4.2.3 Discussion: Advantages of Incorporating Personalization and Biomechanical Simulation. The results of E1 revealed that TelePulse provides more accurate control over muscle activation and more precisely calculates the muscle stimulation required for simulating force directions compared to the conventional method of proportionally delivering EMS intensity based on the force measured by

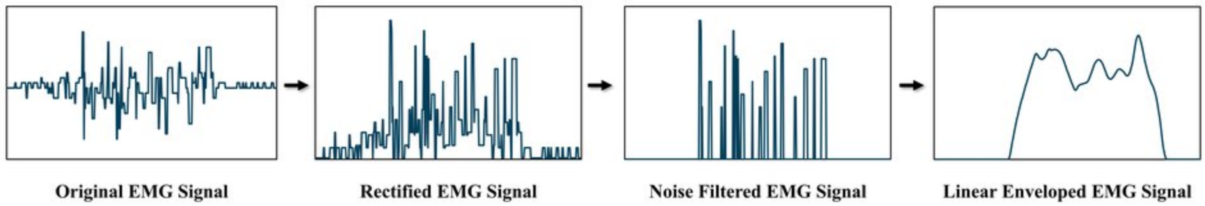

Figure 8: Processing stages of the EMG signal used for comparison with EMS signals. The four panels show (from left to right) the original EMG signal, the rectified EMG signal, the noise-filtered EMG signal, and the linear enveloped EMG signal.

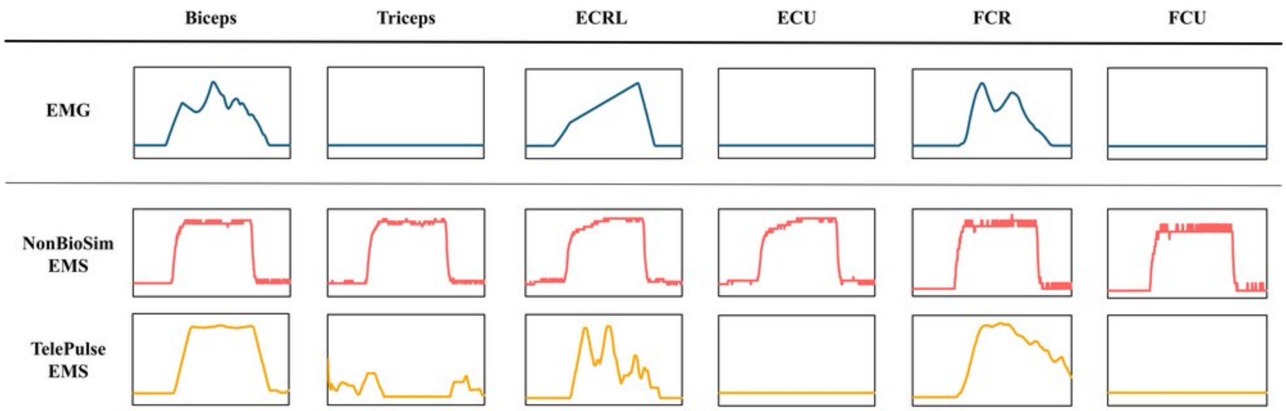

Figure 9: Comparison of EMS signals generated by TelePulse and *NonBioSim* with the corresponding EMG signals across six muscles: biceps, triceps, ECRL, ECU, FCR, and FCU.

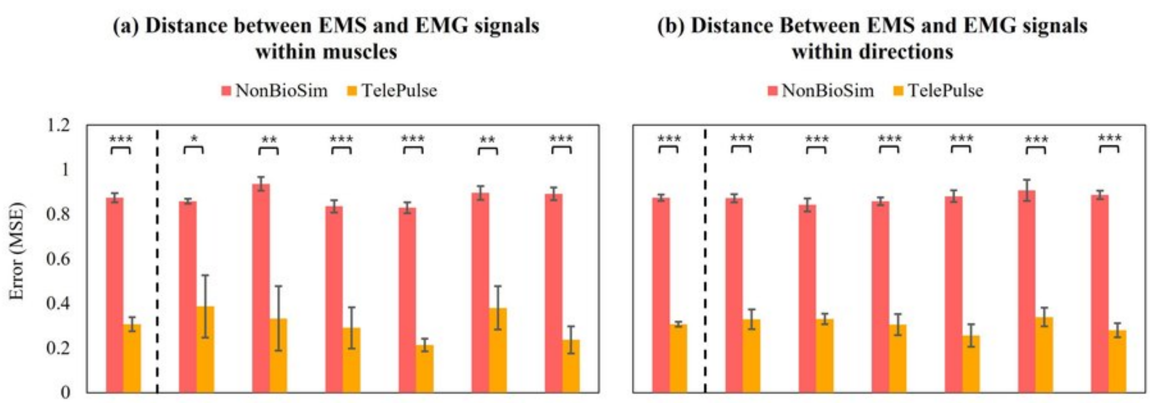

		Total	Biceps	Triceps	ECRL	ECU	FCR	FCU	Total	Left	Right	Up	Down	Forward	Backward
NonBioSim	*M*	0.873	0.858	0.936	0.836	0.829	0.895	0.891	0.874	0.872	0.842	0.858	0.881	0.907	0.886
	SE	0.021	0.012	0.031	0.028	0.025	0.031	0.029	0.014	0.018	0.029	0.017	0.025	0.048	0.019
TelePulse	*M*	0.307	0.387	0.333	0.291	0.214	0.380	0.230	0.317	0.329	0.331	0.306	0.257	0.339	0.280
	SE	0.032	0.140	0.144	0.092	0.028	0.097	0.061	0.011	0.044	0.023	0.048	0.028	0.050	0.042

Figure 10: Distance between EMS and EMG signals. (a) Error between EMS and EMG signals across different muscles. (b) Error between EMS and EMG signals across different force directions. TelePulse consistently shows lower error compared to *NonBioSim*, indicating higher precision in muscle stimulation and force direction rendering. Significance levels: $^{*}p < .05$, $^{**}p < .01$, $^{***}p < .001$.

the F-T sensor. There are two primary factors for the enhanced performance of TelePulse:

Accurate Simulation of Muscle Characteristics: TelePulse determines EMS intensity by considering the unique muscle characteristics of each participant. The system is optimized through a personalization process that estimates the joint torque of the arm based on EMS intensity specific to each individual. The conventional method (*NonBioSim*), which omits personalization of the torque generated by each muscle in response to stimulation, calculates EMS intensity solely from the force measured by the F-T sensor, using linear interpolation between minimum and maximum EMS intensities. In contrast, TelePulse estimates the required EMS intensity by accounting for the user's muscle characteristics, allowing for a more precise simulation of muscle stimulation.

Torque Calculation through Biomechanical Simulation: TelePulse incorporates biomechanical simulation to estimate the required torque for each joint based on the user's pose and the forces applied to the robotic manipulator. This allows TelePulse to selectively stimulate only the necessary muscles for the given force directions. In contrast, *NonBioSim*, which does not incorporate biomechanical simulation and lacks information about the operator's biomechanical properties, cannot differentiate which muscles to activate. This difference is particularly evident in Fig. 9, where the activation graphs for the biceps and triceps are shown. According to the EMG analysis, the participant primarily activates the biceps in response to external force on the arm, while the triceps remain inactive. TelePulse correctly calculates that the biceps should be more activated, minimizing stimulation to the triceps. Without these considerations, *NonBioSim* applies EMS equally to both biceps and triceps because it lacks information about the user's pose (e.g., whether the arm is extended, flexed, or raised). This discrepancy demonstrates the reasons TelePulse achieves better performance by using biomechanical simulation to calculate EMS signals.

5 Experiment 2: Live-User Study - Examining TelePulse System's Effect on Teleoperation Tasks (E2)

5.1 Evaluation Setup

In E1, we validated the accuracy of the EMS intensity calculated by the TelePulse system's personalization and biomechanical simulation. This section details the evaluation of the TelePulse system across two teleoperation tasks: the *Sanding Task* and the *Drilling Task*, to examine the following two aspects: 1) how effectively it improved task performance by providing virtual forces during teleoperation, and 2) how much it enhanced user presence during the teleoperation tasks.

Task Setup and Comparison Conditions. In this study, we categorized the forces acting on a user's arm during teleoperation into two main types: continuous force and impulse force. Continuous forces involve sustained pressure on the arm over a prolonged period, such as when pressing a board with the robotic arm during a sanding task or when holding and moving an object with constant weight. In these scenarios, the user's arm continuously moves while the haptic feedback adjusts in real-time to provide sustained force feedback through controlled EMS intensities and targeted muscles. Conversely, impulse forces are short-duration forces that are applied and removed quickly, such as when hammering a nail or drilling through a material. In these cases, the intensity and targeted muscles of the stimulation are determined based on the user's posture, joint angular velocity, and angular acceleration at that moment.

Based on these classifications, we designed two separate teleoperation tasks to observe whether TelePulse could improve task performance in teleoperation and how user experience would differ. The first teleoperation task, the "*Sanding Task*," was designed to assess the system's ability to provide continuous force feedback while sanding a large wooden board. The second teleoperation task, the "*Drilling Task*," was created to evaluate the system's capability to provide impulse force feedback during the drilling of multiple wooden boards.

In our study, participants were introduced to four distinct haptic stimulation conditions. The first condition, labeled **Baseline**, was a control condition in which participants did not receive any haptic stimulation. To exclude variations in user experience due to wearing the device and to maintain the calibrated EMS electrode positions, the participants wore the equipment, but no stimulation was provided. In the second condition, labeled **NonBioSim**, EMS was applied without incorporating biomechanical simulation calculations. Instead, the stimulation intensity was mapped proportionally to the maximum force the robotic arm could exert (30 N) and the participant's pain threshold (I_{PT}), with the stimulus intensity increasing proportionally to the F-T sensor readings. We included the **NonBioSim** condition to test the role of biomechanical simulation in force feedback, using EMS intensity scaled solely by measured force without biomechanical modeling. This allowed us to investigate the impact of incorporating biomechanical simulation by comparing TelePulse's simulation-based EMS approach to an EMS method that simply scaled stimulation intensity in direct proportion to the measured force, without considering user posture or biomechanical details. The third condition, labeled **TelePulse**, applied haptic force feedback via EMS based on biomechanical simulation calculations. The fourth condition, labeled **ElecTac**, provided tactile sensations without inducing muscle contractions by adjusting the electrical stimulation frequency to 20 Hz, following Pamungkas et al.'s study [89]. In contrast, as explained in Section 3.5, the EMS conditions used a 100 Hz frequency to ensure muscle contractions, which typically occur at EMS frequencies above 50 Hz [41, 55]. Identical to Pamungkas et al.'s study [89], this condition did not involve biomechanical simulations and used a stimulus intensity proportional to the F-T sensor values. The **ElecTac** condition was chosen to compare TelePulse's EMS-based force simulation with a commonly used electrotactile approach that does not produce muscle contractions, providing only surface-level tactile cues. By comparing these conditions, we assessed whether TelePulse could enhance task performance during teleoperation and improve the user's experience.

User Presence and Experience Evaluation Setup. We used the Witmer-Singer presence questionnaire [116] to assess the user's level of presence across different environments and conditions. This questionnaire comprises a total of 32 items and employs a 7-point Likert scale to collect responses from participants. For a detailed understanding of our survey and assessment criteria, we have included the full set of questionnaire items used in our experiment in Appendix B. The questionnaire categorizes the user's sense of presence into four factors as follows:

- **Control Factor**: This factor assesses the user's capability to interact with and manage elements within the virtual environment. It examines the level of immediate responsiveness of the environment to the user's actions and the extent of control that the user perceives. A greater sense of control can amplify the user's feeling of presence.
- **Sensory Factor**: This factor evaluates the sensory information provided by the virtual environment in terms of quality and consistency, including the level of engagement provided by the visual, auditory, and tactile experiences. The more convincing and encompassing these sensory inputs are, the more present a user is likely to feel.
- **Distraction Factor**: This factor evaluates the degree to which distractions disrupt the user's experience within the virtual environment. Distractions may impede the user's immersion and diminish their sense of presence. These distractions include external factors, such as noise from the physical environment, as well as internal factors, such as discomfort or awareness of the equipment being used.
- **Realism Factor**: This factor assesses the extent to which the virtual environment appears realistic to the user. It reflects how closely the environment mirrors real-world experiences and behaviors. The more realistic the environment, the more likely the user is to feel immersed in it.

Furthermore, we conducted open-ended interviews to investigate the detailed user experiences. The structure of the interview questions is as follows:

- How did the haptic feedback provided by TelePulse affect your experience of performing the teleoperation task?
- How closely did the haptic feedback from TelePulse resemble a real-life experience?
- Which elements of the teleoperation task did you find particularly immersive? Or were there any elements that prevented immersion?

All participants were recruited under the same participant conditions as in E1, and the study was conducted with a total of eight participants (age range: 22 − 25 years, M = 24.13, SD = 1.25, 5 males, 3 females). Among these participants, three had no prior experience with EMS, while nine had experience using EMS in physical therapy devices. However, none of the participants had previously used EMS for haptic stimulation. All experimental conditions were randomized using a Latin-square design. Before the experiment began, all participants completed the personalization process outlined in Section 3.2 and were instructed to take sufficient breaks between experiments. To ensure the validity of EMS personalization, participants maintained the same electrode placement for the personalization process and the entirety of E2. The study received approval from the Institutional Review Board.

5.2 Teleoperation Task 1: Sanding Task

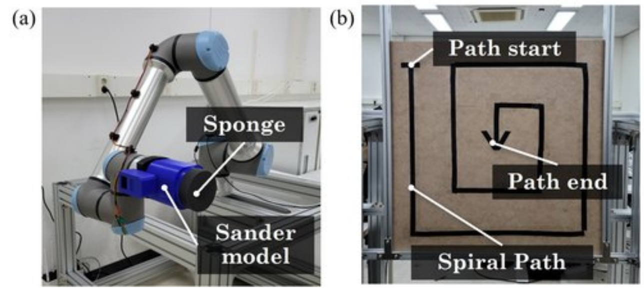

Figure 11: Experimental setup for the sanding task. (a) Robotic arm equipped with a sander model made of sponge and 3D-printed materials. (b) The wooden board with a predefined spiral sanding path, marked with the start and end points of the path.

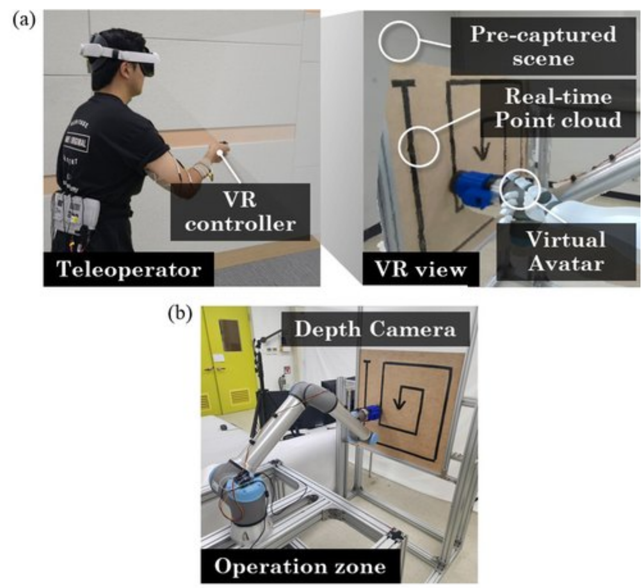

Figure 12: Teleoperation sanding task overview. (a) The teleoperator using a VR controller to guide the robotic arm and VR view displaying real-time point cloud data and pre-captured scene. (b) Operation zone showing the robotic arm with a sander and depth camera setup.

5.2.1 Task Setup and Procedure. The first teleoperation task involved remotely controlling a robotic arm equipped with a sander to evenly sand a wooden board. In this task, participants used a VR controller to move the robotic arm's end-effector, which was synchronized with the controller's position, to follow a predefined spiral path on the wooden board (Fig. 11 (b)). Within the VR environment, participants could observe the teleoperation zone in real-time through a point cloud representation generated by a depth camera (Fig. 12 (b)), allowing them to monitor the movement of the robotic arm and the sanding process. For the static background, a pre-captured 3D reconstructed operation zone was used to enhance realism (Fig. 12 (a)). For safety reasons, a sander model made of sponge and 3D-printed materials was used in the experiment (Fig. 11 (a)).

During the sanding task, participants received continuous force feedback corresponding to the force applied during sanding. The intensity and direction of this force feedback varied depending on factors such as the depth of the sander's pressure, the friction generated along the sanding path, and the robot manipulator's posture and position. In all conditions, before the experiment began, participants completed a 2-minute practice session to familiarize themselves with the reference sanding force (15 N). In the main experiment, participants were instructed to maintain this reference force while following the spiral path. To prevent safety hazards and potential damage to the robot, a warning message was displayed if the force applied to the robotic arm's end-effector exceeded 30 N, ensuring that the force remained below this threshold. The sanding task was performed twice under each condition, resulting in a total of 8 trials (4 conditions $\times$ 2 trials). The experiment followed a within-subject design, and the order of conditions was counterbalanced across participants. During the experiment, data including the participants' upper body motion capture, the position of the robotic arm's end-effector, and the force applied to the robotic arm were collected in real-time for subsequent analysis.

5.2.2 Results of the Sanding Task.

Teleoperation Task Performance Results: We measured task performance in the continuous force application task by asking participants to sand a wooden board along a predetermined path, with the pressure data along the path displayed as a heatmap in Fig. 13. We analyzed how consistently participants maintained the reference force while sanding by calculating the Mean Absolute Error (MAE) between the reference force and the recorded vertical force, which is shown in Fig. 14. In this figure, the x-axis represents each experimental condition, while the y-axis denotes the MAE between the reference force and the recorded vertical force. For all conditions, the absolute values of skewness and kurtosis did not exceed 3.0 and 10.0, respectively; therefore, normality was satisfied [53]. We conducted a one-way repeated measures ANOVA (RM ANOVA) to analyze the impact of TelePulse on the consistency of force application, and detailed results can be found in Table. 3 in Appendix A. For all force application measures, the assumption of sphericity was tested using Mauchly's test. If sphericity was not satisfied, we used the Greenhouse-Geisser correction for degrees of freedom. For pairwise comparisons, we conducted a post-hoc test using the Bonferroni correction.

The experimental results showed that under the TelePulse condition, participants were able to maintain the reference force with significantly less error compared to all other conditions. In contrast, the *NonBioSim* and *ElecTac* conditions recorded less error than the *Baseline*, but the differences were not statistically significant. This suggests that biomechanical simulation played a major role in enhancing task performance in the continuous force application task. TelePulse, which allowed participants to perceive both the direction and magnitude of the force from the remote robotic manipulator, enabled them to distinguish between the vertical force needed for sanding and the horizontal force needed for path progression. However, in the *NonBioSim* and *ElecTac* conditions, participants could only perceive the magnitude of the force without distinguishing between the different directional forces, making it more challenging to maintain the vertical force consistently with the reference.

TelePulse's influence on user presence: The results from the Witmer-Singer presence questionnaire for the sanding task are shown in Fig. 15. The x-axis represents the overall presence score and the four subscales of presence, while the y-axis denotes the presence score normalized on a 7-point Likert scale with a standard deviation. For all conditions, the absolute values of skewness and kurtosis did not exceed 3.0 and 10.0, respectively; therefore, normality was satisfied [53]. We conducted a one-way RM ANOVA to analyze the impact of TelePulse on each element of presence, and detailed results can be found in Table. 3 in Appendix A. For all presence subscales, the assumption of sphericity was tested using Mauchly's test. If sphericity was not satisfied, we used the Greenhouse-Geisser correction for degrees of freedom. For pairwise comparisons, we conducted a post-hoc test using the Bonferroni correction.

In the task requiring continuous force application while sanding a wooden board, the TelePulse condition recorded the highest presence, followed by *ElecTac*, *NonBioSim*, and *Baseline*. All stimuli, when compared to the *Baseline*, did not significantly increase user distraction (Distraction factor) and led to higher levels of immersion through sensory stimulation (Sensory factor). Specifically, the *ElecTac* and TelePulse conditions produced higher presence due to more realistic stimuli (Realism factor), and in the case of TelePulse, biomechanical simulation provided participants with more immediate and higher control compared to the *NonBioSim* condition (Control factor). This indicates that TelePulse's biomechanical simulation offered users greater control in the continuous force application task and provided a similar or even higher level of realism and sensory alignment compared to traditional electrotactile stimulation.

5.3 Teleoperation Task 2: Drilling Task

5.3.1 Task Setup and Procedure.

The second teleoperation task involved remotely controlling a robotic arm equipped with a drill to perform a drilling operation on wooden boards. In this task, the remote operator used a VR controller to move the robotic arm's end-effector, synchronized with the controller's position, to drill through exactly two of the three stacked wooden boards. The distance between the first and third boards was set to 3 cm, while the middle board was randomly positioned either 1 cm or 2 cm away from the first board (Fig. 16 (b)). This random placement was intended to prevent participants from estimating and learning the location of the second board, thereby ensuring that they relied on haptic feedback to detect the contact and breakthrough moments. By designing the task to minimize learning effects and emphasize haptic sensations, we aimed to allow the results of the experiment to be more influenced by the haptic feedback provided by each system. Since our primary goal was to understand the differences in user experience resulting from the haptic feedback of the three systems (*Electac*, *NonBioSim*, *TelePulse*), and these systems provided feedback conveying the force information of drilling through a wooden board in different ways, we aimed for a comparison focused on haptic input. The drill attached to the end-effector of the robotic arm could be triggered by a servo motor (Fig. 16 (a)), which was activated by pressing the trigger button on the VR controller (Fig. 17 (a)).

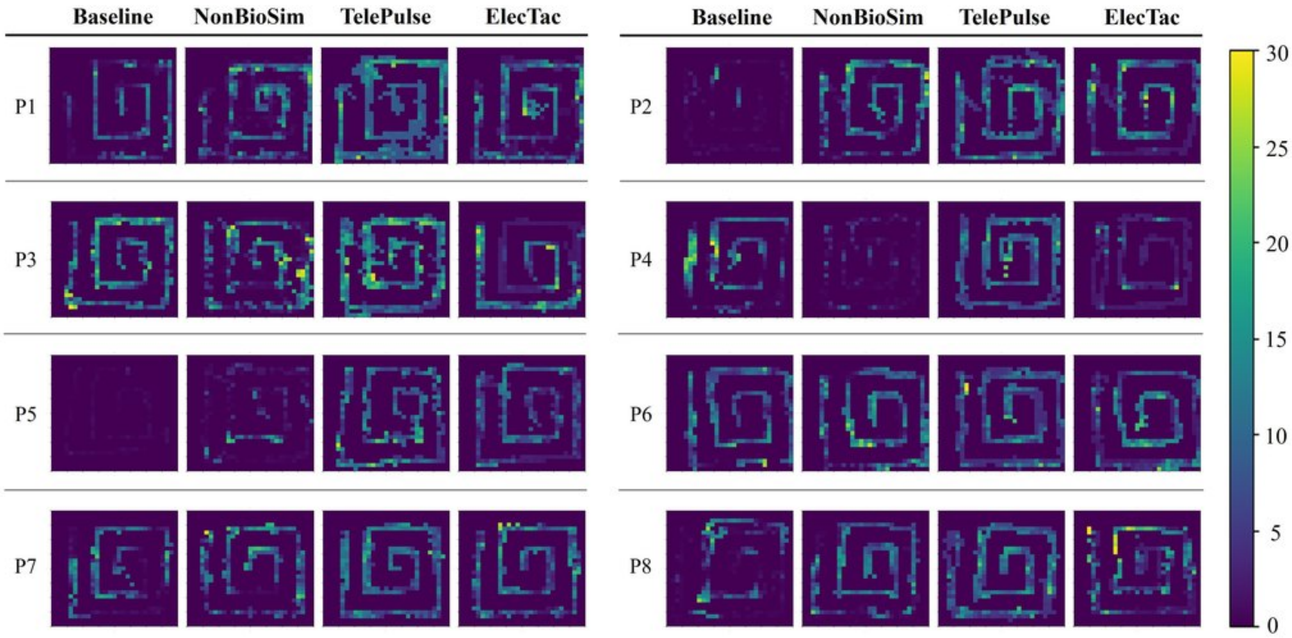

Figure 13: Heatmap visualization of the average sanding force applied across different positions on the board by eight participants (*P1–P8*) under four different conditions: *Baseline, NonBioSim*, TelePulse, and *ElecTac*.

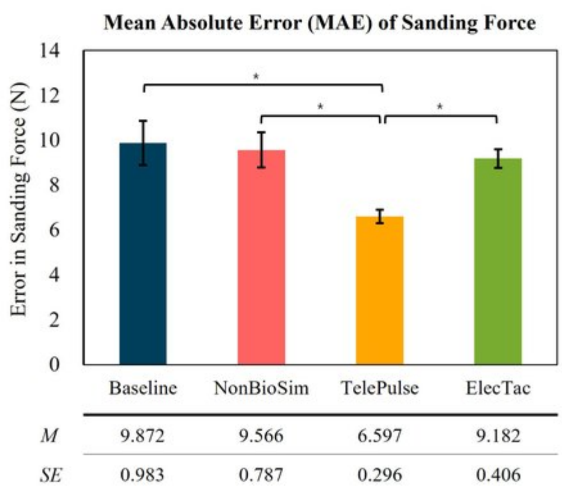

Figure 14: Mean Absolute Error (MAE) of sanding force across four conditions: *Baseline, NonBioSim*, TelePulse, and *ElecTac*. The y-axis represents the error in sanding force (N), calculated as the MAE relative to the reference force of 15 N. Significance levels are indicated: $^{*}p < .05$.

During the drilling task, the remote operator experienced momentary impulse force feedback when the drill contacted the wooden boards and when it broke through them. The intensity and direction of this force feedback varied depending on factors such as the direction and speed of the drill's contact with the boards, and the posture and position of the robotic manipulator. Before starting the main experiment, participants completed a 2-minute practice session to familiarize themselves with the drilling task. The drilling task was performed twice under each condition, resulting in a total of 8 trials (4 conditions × 2 trials). The experiment followed a within-subject design, and the order of conditions was counterbalanced across participants. During the experiment, data including the participants' upper body motion capture, the position of the robotic arm's end-effector, and the force applied to the robotic arm were collected in real-time for subsequent analysis.

5.3.2 Results of the Drilling Task.

Teleoperation Task Performance Results: The task performance of applying impulse force to drill through only two out of three wooden boards showed the results depicted in the Fig. 18. The results were recorded as follows: ***1*** for cases where the drill completely penetrated the board, creating a hole; ***0.5*** for cases where the drill made contact with the board, causing scratches or dents but not fully penetrating it; and ***0*** for cases where the drill did not touch the board at all. To determine the accuracy with which participants performed the remote task on average, we compared the interquartile range (IQR) between the 25th and 75th percentiles. The results showed that TelePulse, *ElecTac*, *Baseline*, and *NonBioSim* exhibited progressively wider IQRs. These findings confirmed that TelePulse supported remote operators in drilling through only two wooden boards with greater accuracy and less variance compared to other conditions. Furthermore, it was confirmed that electrotactile feedback, widely used in previous studies, also improved task accuracy compared to the baseline. On the other hand, EMS

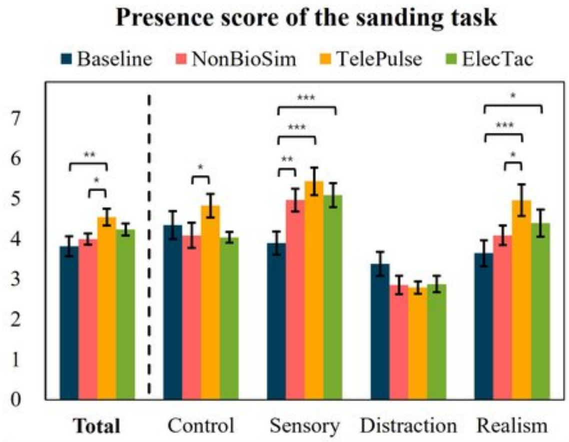

	Total	Control	Sensory	Distraction	Realism
Baseline					
M	3.815	4.346	3.898	3.375	3.643
SE	0.247	0.350	0.287	0.298	0.327
NonBioSim					
M	3.999	4.087	4.966	2.854	4.089
SE	0.139	0.314	0.282	0.226	0.247
TelePulse					
M	4.540	4.827	5.432	2.792	4.964
SE	0.207	0.292	0.340	0.153	0.397
ElecTac					
M	4.236	4.038	5.091	2.875	4.393
SE	0.150	0.133	0.298	0.204	0.333

Figure 15: Results from Witmer-Singer presence questionnaire for "*Sanding Task*". The x-axis displays the five presence factors, comparing scores based on the *Baseline*, *NonBioSim*, TelePulse and *ElecTac* conditions. The y-axis represents participants' responses, which have been normalized on a 7-point Likert scale. Significance levels are indicated: $^{*}p < .05$, $^{**}p < .01$, $^{***}p < .001$.

stimulation without biomechanical simulation reduced task accuracy compared to when no stimulation was applied. This implies that accurate biomechanical simulation played a major role in enhancing the remote task support capabilities of TelePulse, and that without precise simulation, remote task performance may actually be hindered.

TelePulse's influence on user presence: The results from the Witmer-Singer presence questionnaire for the drilling task are shown in Fig. 19. The x-axis represents the overall presence score and the four subscales of presence, while the y-axis denotes the presence score normalized on a 7-point Likert scale with a standard deviation. For all conditions, the absolute values of skewness and kurtosis did not exceed 3.0 and 10.0, respectively; therefore, normality was satisfied [53]. We conducted a one-way RM ANOVA to analyze the impact of

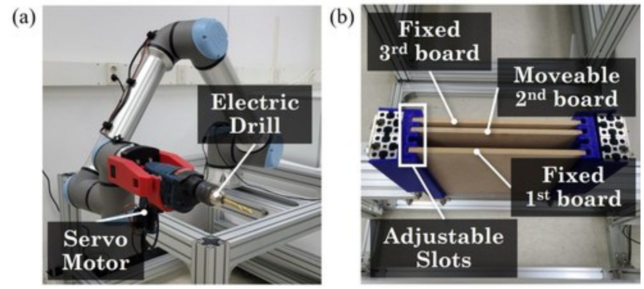

Figure 16: Experimental setup for the drilling task. (a) Robotic arm equipped with an electric drill and servo motor for triggering. (b) Adjustable slots holding three wooden boards in place, with the middle board moveable to vary the drilling depth.

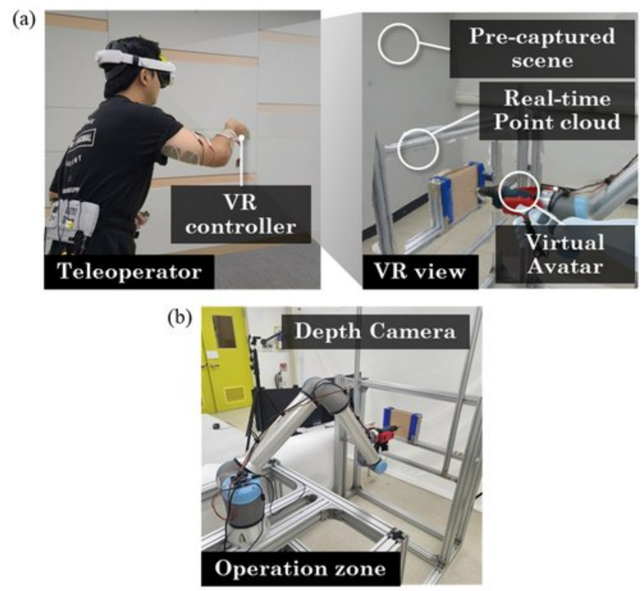

Figure 17: Overview of the teleoperation drilling task. (a) The teleoperator uses a VR controller to control the robotic arm, activating the drill via the trigger and VR view shows real-time point cloud data and a pre-captured scene of the environment. (b) The operation zone setup, with the robotic arm equipped with a drill, monitored by a depth camera.

TelePulse on each element of presence in the drilling task; detailed results can be found in Table. 4 in Appendix A. For all presence subscales, the assumption of sphericity was tested using Mauchly's test. If sphericity was not satisfied, we used the Greenhouse-Geisser correction for degrees of freedom. For pairwise comparisons, we conducted a post-hoc test using the Bonferroni correction.

In the *drilling task*, which requires the application of strong impulsive force, it was observed that participants experienced significantly higher total presence under the TelePulse condition compared to all other conditions. All stimuli, when compared to the

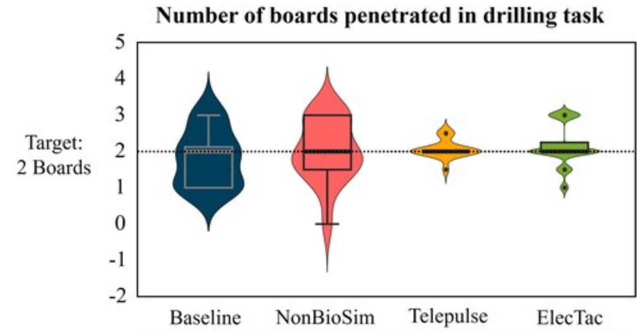

	Baseline	NonBioSim	Telepulse	ElecTac
M	1.813	2.000	2.063	2.125
SD	0.772	0.856	0.250	0.592
Min	1.000	0.000	1.500	1.000
Max	3.000	3.000	2.500	3.000
25th percentile	1.000	1.500	2.000	2.000
75th percentile	2.125	3.000	2.000	2.250
IQR	1.125	1.500	0.000	0.250

Figure 18: Box plot and violin plot displaying the number of boards penetrated in the drilling task across four conditions: *Baseline, NonBioSim,* TelePulse, and *ElecTac.* The y-axis represents the number of boards penetrated, with a target value of 2 boards indicated by the dashed horizontal line.

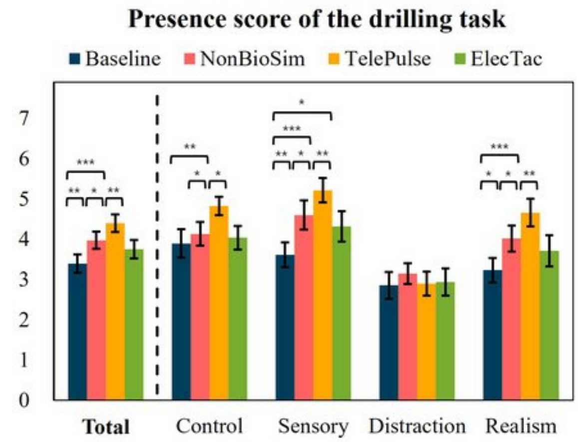

		Total	Control	Sensory	Distraction	Realism
Baseline						
	M	3.399	3.894	3.614	2.854	3.232
	SE	0.230	0.352	0.306	0.328	0.304
NonBioSim						
	M	3.975	4.135	4.602	3.146	4.018
	SE	0.211	0.294	0.366	0.261	0.322
TelePulse						
	M	4.400	4.827	5.216	2.896	4.661
	SE	0.217	0.226	0.304	0.297	0.342
ElecTac						
	M	3.752	4.038	4.318	2.938	3.714
	SE	0.231	0.296	0.377	0.341	0.386

Figure 19: Results from Witmer-Singer presence questionnaire for "*Drilling Task*". The x-axis displays the five presence factors, comparing scores based on the *Baseline, NonBioSim,* TelePulse and *ElecTac* conditions. The y-axis represents participants' responses, which have been normalized on a 7-point Likert scale. Significance levels are indicated: $^{*}p < .05$, $^{**}p < .01$, $^{***}p < .001$.

baseline, did not cause significant additional distraction, confirming that the stimuli did not lead to increased attentional dispersion. TelePulse demonstrated higher levels of immediate responsiveness (Control factor), enhanced immersion through quality sensory stimulation (Sensory factor), and allowed for a more realistic virtual environment experience without causing additional distractions (Distraction factor) compared to all other conditions. Meanwhile, the electrotactile stimulation provided a higher sensory match than the baseline but was less effective compared to other conditions in terms of the sense of system control and realism compared to other conditions. Lastly, the EMS stimulation without biomechanical simulation induced a higher sensory match and greater realism but was less effective than TelePulse in terms of immediate responsiveness and the resulting sense of control over the system.

5.4 Discussion: Analysis of the Interview

In this study, we evaluated task performance and user experience in two teleoperation environments: continuous force tasks and impulsive force tasks. In both environments, TelePulse provided users with higher task performance and a greater sense of presence compared to other conditions. To gain deeper insights into user experience, we conducted interviews for each condition (Table. 1).

Across both tasks, users reported that the TelePulse condition allowed them to clearly perceive both the direction and magnitude of the force *(P1-8)*. They were able to distinctly recognize when the force changed during the remotely operated robotic manipulator's interaction with the work environment, the application of force, and throughout task execution. Additionally, users noted that the biomechanical simulation of TelePulse, which stimulates only the appropriate muscles, provided more realistic and predictable force feedback compared to other conditions *(P2, P5-7)*. This alignment of haptic feedback with visual information was said to positively influence the sense of presence in the teleoperation environment, and these results were consistent with teleoperation studies that provided haptic stimuli combined with visual information [114]. Furthermore, *P8* mentioned that they could feel the inertia of the equipment held by the robotic manipulator, as well as the resulting load. This allowed them to choose manipulation methods that reduced the load on the robot, thereby increasing the degree of freedom in task execution, demonstrating the effectiveness of TelePulse's biomechanical simulation.

Compared to the *NonBioSim* condition, users indicated that TelePulse selectively actuated only the necessary muscles in the arm, thereby avoiding the sensation of stiffness and enabling for

Table 1: Interview responses from participants who experienced the TelePulse system. Responses for each task are categorized as positive or negative.

	Positive Feedback	Negative Feedback
Sanding	I could really tell when the force was getting stronger or weaker, and I could also feel the direction it was coming from during the sanding task. *(P1-8)*	I noticed a slight delay compared to other systems. *(P6)*
	When the sander touched the board, the force felt much more realistic compared to other systems. *(P2, P5-7)*	There was so much information, like the force intensity and direction, that sometimes it made sanding harder. *(P6-7)*
	It was nice that only the necessary muscles were stimulated. It didn't make my arm feel stiff, so I wasn't distracted by the haptics while sanding. *(P2, P5, P7)*	Like in *NonBioSim*, I still felt that tingling sensation, which was a bit uncomfortable. *(P1, P6)*
	Compared to *ElecTac*, the detailed force feedback helped judge the sander's progress in real-time. *(P2-5)*	I thought the force feedback wasn't as realistic as with *NonBioSim*, which gave stronger stimulation. *(P8)*
Drilling	I could clearly feel the strength and direction of the drill's impact when it hit the wood. *(P1-8)*	There was a small delay compared to the other conditions. *(P6)*
	I actually felt the inertia of the drill and the load it created. *(P8)*	That tingling sensation, like in *NonBioSim*, was still a bit uncomfortable. *(P1, P6)*
	With TelePulse, I didn't have the problem of all my muscles being activated like with *NonBioSim*, which made the drilling task a lot smoother. *(P7)*	I think *NonBioSim* did a better job of making the drilling feel more realistic, especially when it came to the strong impacts on my arm. *(P3, P8)*
	With the *ElecTac*, it felt more like a vibration, and I couldn't tell if the sensation was from the drill's vibration or the force feedback. But with TelePulse, I didn't have that confusion. *(P2-3, P5)*	

more delicate manipulations by preventing unintended muscle actuation *(P2, P5, P7)*. *P7* reported that the overall muscle actuation in the *NonBioSim* condition made task performance challenging, an issue they did not encounter with TelePulse. When compared to electrotactile stimulation, users stated that TelePulse provided a clearer perception of force, which conveyed more information about the task environment *(P2-5)*. Specifically, participants mentioned that electrotactile stimulation felt more like a vibration, making it difficult to distinguish whether the sensation was due to equipment vibration or a haptic cue representing force magnitude *(P2-3, P5)*.

In addition to these positive responses, the interviews also revealed areas for improvement in TelePulse. Some users reported a slight delay in TelePulse compared to other conditions *(P6)*, suggesting that the computation time required for biomechanical simulation could negatively impact the experience. This delay could potentially be mitigated through algorithm optimization and increased computing power. Additionally, due to the wide range of information provided by TelePulse, some users found it challenging to concentrate on the task *(P6-7)*. This issue could be addressed by selectively limiting the amount of information provided based on user preferences (e.g., simplifying visual information or filtering the direction and magnitude of force feedback). Furthermore, both TelePulse and *NonBioSim* EMS stimulation were reported to cause tingling sensations due to the electrical stimulation, which some participants found uncomfortable *(P1, 6)*. This is a common limitation of EMS haptic systems but could be alleviated by adjustments in stimulation settings or exploring alternative methods, such as magnetic muscle stimulation [107], which may reduce tingling sensations.

When compared to *NonBioSim*, some participants found TelePulse to be less realistic *(P8)*. Specifically, this feedback was noted during the drilling task *(P3, P8)*, where strong impacts were expected. Participants reported that *NonBioSim* was more effective in conveying the sensation of strong impacts throughout the arm, which they felt more closely resembled the actual experience of using a drill. However, the results of the Witmer-Singer presence questionnaire indicated that TelePulse had the highest realism factor among all conditions. This suggests that the issue may be specific to certain participants and could potentially be addressed by fine-tuning the intensity of the stimuli. Lastly, when compared to electrotactile stimulation, some participants noted that the real force provided by TelePulse led to muscle fatigue, making it more challenging to control the manipulator in the desired direction *(P3)*. We expect that this could also be resolved by personalizing the intensity of the TelePulse stimulation and adjusting the force scale based on the task or the performance of the robotic manipulator.

6 Discussion

RQ1: How accurately can TelePulse replicate natural muscle activations using biomechanical simulations and EMS during force-directed teleoperation tasks?

TelePulse utilizes body tracking through the *Meta Quest 3* to measure the user's posture and calculate the muscle activation required in response to the virtual forces acting on that posture.

Our experiment results confirmed that the EMG patterns of each muscle changed depending on the direction of the applied force in all six directions; accordingly, TelePulse's biomechanical simulation selectively stimulated specific muscles based on posture and force direction. These findings are consistent with prior studies in the fields of rehabilitation and biomechanics [13, 96, 119]. Specifically, Flanders et al.'s report showed that wrist muscle activation varies based on arm position [25], and their subsequent research demonstrated that the phasic and tonic activation waveforms of arm muscles shift with dynamic arm movements [24]. Additionally, Roh et al.'s study revealed that the human nervous system employs a limited number of muscle synergies when exerting force, as seen in the synergy changes of four wrist muscle activation patterns [99]. In our experiment, the EMG patterns and TelePulse's EMS patterns, which varied according to user movement, posture, and the direction of applied force, align with these previous studies, supporting the results of our experiment.

In E1, we instructed participants to apply force in six different directions on the robotic arm. For each direction, we measured muscle activation in six muscles using EMG data, allowing us to observe how arm muscles activated depending on the direction of the force. By comparing these EMG signals with EMS signals, we assessed the precision of the TelePulse system against *NonBioSim*. The results of E1 showed that the EMS signal patterns from TelePulse were consistently closer to the EMG patterns across all six directions compared to *NonBioSim*, demonstrating that TelePulse produced more precise EMS signals due to its ability to identify and stimulate the specific muscles required, based on the biomechanical simulation.

RQ2: Can TelePulse enhance user experience and task performance in teleoperation through biomechanical simulation based EMS?

We conducted experiments in two distinct task environments — continuous force and impulsive force — to investigate whether TelePulse can enhance remote operators' task performance and improve user experience. In the continuous force task, which involved sanding, TelePulse supported users in maintaining the reference force throughout the task. In the impulsive force task, which involved drilling, it allowed participants to precisely control the drill, ensuring it penetrated the desired number of wooden boards. These results demonstrated the superiority of TelePulse over the *NonBioSim* condition, where EMS stimulation was applied without biomechanical simulation, and over the widely used electrotactile stimulation, highlighting the utility of TelePulse.

In terms of user presence with TelePulse, during the drilling task (impulsive force task), all factors—Control, Sensory, and Realism—showed statistically significant improvements compared to the electrotactile system. However, in the sanding task (continuous force task), while TelePulse showed numerically superior results, these were not statistically significant. This indicates that TelePulse's EMS stimulation may provide a more immersive experience in tasks involving impulsive force than continuous force, suggesting that the level of presence induced by TelePulse may vary depending on the type of force involved in the task. Additionally, this result aligns with previous studies using EMS in VR haptic systems. Lopes et al. reported that "repulsion," which provides instantaneous force, can lead to a higher sense of presence than interactions with "hard & soft objects" in continuous force scenarios [72]. In their study, most users reported feeling their arms being pulled back rather than pushing against a hard wall, which negatively impacted the sense of presence. Although this phenomenon was not reported in our interviews, we acknowledge that the level of presence provided by TelePulse could differ depending on the task, and these results are consistent with prior research. This suggests that further research could be conducted to enhance presence in continuous force environments.

However, TelePulse successfully improved users' task performance across all environments, demonstrating its effectiveness in supporting teleoperation. In particular, comparisons with the *NonBioSim* condition showed that TelePulse's biomechanical simulation prevented muscle stiffness and unwanted actuation in unintended directions, leading to improved task performance, an increased sense of presence, and reduced physical task load. Furthermore, compared to traditional electrotactile stimulation [88, 89, 103], TelePulse's EMS-based force simulation provided richer information about the environment, helped users distinguish the target forces through clear directional feedback, and enabled them to perceive the robot's load and limitations, thus increasing task flexibility.

RQ3: What are the limitations of using biomechanical simulations and EMS for haptic feedback in teleoperation, and how can these limitations be mitigated?

In this study, while TelePulse successfully enhanced task performance and overall user experience, the interviews revealed areas for potential improvement. The interviews identified three main limitations of the current TelePulse system: 1) delays in the computational process, 2) decreased concentration due to high information load, and 3) tingling sensations caused by EMS.

First, the computational delay could be mitigated through algorithm optimization and increased computing power. Additionally, most participants did not report discomfort from the delay, and considering the high control factor score of the TelePulse system, it is likely that the alignment between haptic feedback and visual information helped compensate for the perceived delay, giving TelePulse an advantage in responsiveness.

Second, TelePulse provides users with more information about the task environment by delivering both the magnitude and direction of force, which some users found overwhelming, making it difficult to concentrate. This phenomenon has been noted in Weber and Eichberger's meta-analysis [114], which examined the effects of haptic feedback in teleoperation systems. They emphasized that during teleoperation tasks, processing sensory inputs unrelated to the task, often led to decreased task performance and diminished user focus [32, 81, 98]. Similarly, Lathan et al. [59] found that filtering unnecessary sensory information positively influenced teleoperation performance, indicating that performance can be optimized through this approach. Therefore, the TelePulse system could address this issue by filtering and delivering only the task-relevant force information, ensuring that unnecessary force data is excluded. Furthermore, Ziegler et al. [121] demonstrated that external auditory and visual distractions significantly impair task performance in attention-demanding environments. Thus, creating an environment within the TelePulse system that minimizes external distractions (e.g., background noise or visual clutter) could further improve user focus during tasks.

Lastly, the EMS stimulation in TelePulse caused tingling sensations for some users, a common issue with EMS haptic systems. This tingling occurs when electrical pulses pass through the electrode and activate skin receptors before reaching muscle fibers, leading to an unpleasant "buzzing" sensation [50, 86, 92]. This issue is not unique to TelePulse but is common in EMS-based systems [107]. To address this, methods like using biocompatible EMS pads with improved skin adhesion for better signal transmission [60], or using magnetic muscle stimulation [107], which bypasses skin receptors and reduces tingling, could be explored. Incorporating these methods in future iterations of TelePulse could significantly enhance user comfort.

7 Conclusion and Future Works

In this paper, we introduced TelePulse, a haptic feedback system that combines biomechanical simulations with EMS to enhance teleoperation experiences in virtual reality. By leveraging real-time force data from remote manipulators, TelePulse translates these forces into EMS signals that stimulate user muscles, providing natural and precise force feedback. Our system was evaluated across a series of force-directed teleoperation tasks, demonstrating that the EMS signals generated by TelePulse closely matched EMG data, confirming the system's high fidelity in replicating muscle activation and thereby delivering accurate force feedback. Subsequently, this increase in accuracy led to enhanced teleoperation task precision in live user experiments, with participants achieving a 22% reduction in MAE during continuous force tasks, such as sanding, and a 30% improvement in accuracy during impulse force tasks, such as drilling. Furthermore, the use of TelePulse increased user presence in teleoperation environments, reflecting the system's ability to deliver more realistic force feedback. These findings highlight the potential of biomechanical simulation-based EMS systems to transform teleoperation experiences by offering more natural and immersive haptic feedback.

Based on this study, we aim to pursue the following research directions: The system proposed in this study was implemented by targeting only six muscles to ensure rapid computation and ease of electrode attachment. In future research, we intend to stimulate a wider variety of muscles in different locations, enabling higher degrees of freedom in movement and more nuanced force feedback. Specifically, we expect that by integrating a simulation system that includes shoulder and hand muscles, along with additional electrode attachments, we can provide more realistic haptic feedback. Furthermore, we plan to expand the use of biomechanical simulation beyond torque calculation by incorporating a computational muscle model [15, 58, 76] to calculate the activation levels of individual muscles, accounting for voluntary muscle activation in the simulation. The force characteristics of human muscles can vary depending on factors such as muscle fiber and tendon length, contraction and relaxation speed, and fatigue levels [10, 66, 115, 117]. Therefore, future research will aim to improve the simulation performance of TelePulse by integrating a computational muscle model that closely aligns with the actual characteristics of user muscles. Additionally, we anticipate that this computational muscle model will simplify the EMS personalization process. Currently, TelePulse requires the personalization of EMS parameters for each muscle, which takes approximately one hour per person. By integrating a realistic computational muscle model in future research, we expect to reduce the personalization time and enhance the practicality of the system.

Moreover, the TelePulse framework could be applied not only to the serial manipulator used in this study but also to other robotic systems such as robot dogs, submarines, surgical robots, and mobile robots. Although we could not validate the force scaling function of external forces in this study based on participant responses, we anticipate that the scaling function will provide appropriate force feedback to users in various scenarios, especially in cases where the force magnitudes differ significantly from typical human scales. Furthermore, we anticipate that the unique advantages of our system—its lightweight design and mobility, combined with force feedback—will be especially beneficial when integrated with VR locomotion technologies such as redirected walking [52, 61, 97], walking-in-place [48, 49, 80], and omnidirectional treadmills [105]. This combination is expected to provide benefits for mobile robots, enabling them to navigate freely and complete missions in unstructured environments.

In future studies, we will compare our system with a wider range of wearable haptic devices, such as vibration motors [9, 44, 56] and skin stretch mechanisms [1, 17]. Through this comparison, we aim to analyze the advantages and disadvantages of biomechanical simulation-based EMS stimulation relative to various haptic devices. Furthermore, by integrating less-explored feedback modalities in teleoperation—including thermal perception [46, 47], vestibular feedback [36–38], and olfactory stimuli [62, 63]—we aim to uncover new possibilities for haptic feedback in teleoperation.

We believe that this paper serves the following role in the EMS and teleoperation academic fields, align with recent trend in the academic community, where EMS is being explored from deeper perspectives to overcome technical challenges. For instance, Takahashi et al. [106] examine wearability with their EMS-integrated smartwatch; Niijima et al.'s research on muscle synergies [79] introduces subtle techniques for influencing motor movements via EMS; Tanaka et al.'s use of magnetic muscle stimulation [107] focuses on enhancing comfort; and Hwang et al.'s *ErgoPulse* [39] improves the precision of EMS stimulation in scenarios involving complex force applications. In line with these developments, TelePulse explored the potential for interactions between humans and non-human entities through EMS. By extending EMS applications beyond replicating forces from a user-matched virtual avatar in a virtual environment, TelePulse provides a system-level framework and examines its ability to deliver forces originating from non-human entities in the real world. We hope this paper inspires broader adoption of EMS technology across diverse contexts by demonstrating its applicability in real-world environments beyond human-scale scenarios.

Acknowledgments

This work was partially supported by the Ministry of Science and ICT (MSIT), Korea, under the ITRC (Information Technology Research Center) support program (IITP-2024-RS-2024-00436398) supervised by the IITP (Institute of Information & Communications Technology Planning & Evaluation) (50%), the Gwangju Institute of Science and Technology (GIST)–Massachusetts Institute of Technology (MIT) Research Collaboration Grant in 2024 (25%), and the National Research Foundation of Korea (NRF) grant funded by the Korea government (MSIT) (RS-2024-00343397) (25%).

References

[1] Marco Aggravi, Florent Pausé, Paolo Robuffo Giordano, and Claudio Pacchierotti. 2018. Design and evaluation of a wearable haptic device for skin stretch, pressure, and vibrotactile stimuli. *IEEE Robotics and Automation Letters* 3, 3 (2018), 2166–2173.

[2] Arash Ajoudani, Nikolaos G Tsagarakis, and Antonio Bicchi. 2011. Tele-impedance: Preliminary results on measuring and replicating human arm impedance in tele operated robots. In *2011 IEEE international conference on robotics and biomimetics*. IEEE, 216–222.

[3] Leandro Ricardo Altimari, José Luiz Dantas, Marcelo Bigliassi, Thiago Ferreira Dias Kanthack, AC Moraes, and Taufik Abrão. 2012. Influence of different strategies of treatment muscle contraction and relaxation phases on EMG signal processing and analysis during cyclic exercise. *Computational intelligence in electromyography analysis—a perspective on current applications and future challenges* (2012), 97–116.

[4] KP Ayodele, OT Akinniyi, AO Oluwatope, AM Jubril, AO Ogundele, and MA Komolafe. 2021. A Simulator for Testing Planar Upper Extremity Rehabilitation Robot Control Algorithms. *Nigerian Journal of Technology* 40, 1 (2021), 115–128.

[5] Tadej Bajd and Marko Munih. 2010. Basic functional electrical stimulation (FES) of extremities: an engineer's view. *Technology and Health Care* 18, 4-5 (2010), 361–369.

[6] Noah Becker, Erik Gattung, Kay Hansel, Tim Schneider, Yaonan Zhu, Yasuhisa Hasegawa, and Jan Peters. 2024. Integrating Visuo-tactile Sensing with Haptic Feedback for Teleoperated Robot Manipulation. *arXiv preprint arXiv:2404.19585* (2024).

[7] Sara Benham, Minhee Kang, and Namrata Grampurohit. 2019. Immersive virtual reality for the management of pain in community-dwelling older adults. *OTJR: occupation, participation and health* 39, 2 (2019), 90–96.

[8] Massimo Bergamasco, Benedetto Allotta, L Bosio, Luca Ferretti, G Parrini, GM Prisco, Fabio Salsedo, and G Sartini. 1994. An arm exoskeleton system for teleoperation and virtual environments applications. In *Proceedings of the 1994 IEEE International Conference on Robotics and Automation*. IEEE, 1449–1454.

[9] Joao Bimbo, Claudio Pacchierotti, Marco Aggravi, Nikos Tsagarakis, and Domenico Prattichizzo. 2017. Teleoperation in cluttered environments using wearable haptic feedback. In *2017 IEEE/RSJ International Conference on Intelligent Robots and Systems (IROS)*. IEEE, 3401–3408.

[10] Jacques Bobet and Richard B Stein. 1998. A simple model of force generation by skeletal muscle during dynamic isometric contractions. *IEEE transactions on biomedical engineering* 45, 8 (1998), 1010–1016.

[11] BG Boyle, RS McMaster, and J Mixon. 1995. Teleoperation of an underwater robotic repair system using graphical simulation. (1995).

[12] Alie J Buckmire, Danielle R Lockwood, Cynthia J Doane, and Andrew J Fuglevand. 2018. Distributed stimulation increases force elicited with functional electrical stimulation. *Journal of neural engineering* 15, 2 (2018), 026001.

[13] S. Carlsöö. 1961. The static muscle load in different work positions : an electromyographic study. *Ergonomics* 4 (1961), 193–211. https://doi.org/10.1080/00140136108930520

[14] Bo Chen, Rui-Qi Liang, Ru-Yan Chen, and Fang-yuan Xu. 2021. The effect of virtual reality training on the daily participation of patients: A meta-analysis. *Complementary Therapies in Medicine* 58 (2021), 102676.

[15] Ernest J Cheng, Ian E Brown, and Gerald E Loeb. 2000. Virtual muscle: a computational approach to understanding the effects of muscle properties on motor control. *Journal of neuroscience methods* 101, 2 (2000), 117–130.

[16] Janelle P Clark, Gianluca Lentini, Federica Barontini, Manuel G Catalano, Matteo Bianchi, and Marcia K O'Malley. 2019. On the role of wearable haptics for force feedback in teleimpedance control for dual-arm robotic teleoperation. In *2019 International Conference on Robotics and Automation (ICRA)*. IEEE, 5187–5193.

[17] Nicoletta Colella, Matteo Bianchi, Giorgio Grioli, Antonio Bicchi, and Manuel G Catalano. 2019. A novel skin-stretch haptic device for intuitive control of robotic prostheses and avatars. *IEEE Robotics and Automation Letters* 4, 2 (2019), 1572–1579.

[18] Ze Cui, Peng Bao, Hao Xu, Mengyu Gong, Kui Li, Saishuai Huang, Zenghao Chen, and Hongbo Zhang. 2021. A study of force feedback master-slave teleoperation system based on biological tissue interaction. In *Intelligent Life System Modelling, Image Processing and Analysis: 7th International Conference on Life System Modeling and Simulation, LSMS 2021 and 7th International Conference on Intelligent Computing for Sustainable Energy and Environment, ICSEE 2021, Hangzhou, China, October 22–24, 2021, Proceedings, Part I 7*. Springer, 134–144.

[19] Scott L Delp, Frank C Anderson, Allison S Arnold, Peter Loan, Ayman Habib, Chand T John, Eran Guendelman, and Darryl G Thelen. 2007. OpenSim: open-source software to create and analyze dynamic simulations of movement. *IEEE transactions on biomedical engineering* 54, 11 (2007), 1940–1950.

[20] Wilfred Taylor Dempster et al. 1955. *Space requirements of the seated operator: geometrical, kinematic, and mechanical aspects of the body with special reference to the limbs*. Vol. 159. Wright Air Development Center Wright-Patterson Air Force Base, Ohio.

[21] Ahmed Elsharkawy, Aya Ataya, Dohyeon Yeo, Minwoo Seong, Seokhyun Hwang, Joseph DelPreto, Wojciech Matusik, Daniela Rus, and SeungJun Kim. 2024. Adaptive In-Vehicle Virtual Reality for Reducing Motion Sickness: Manipulating Passenger Posture During Driving Events. In *Companion of the 2024 on ACM International Joint Conference on Pervasive and Ubiquitous Computing*. 832–836.

[22] Ahmed Ibrahim Ahmed Mohamed Elsharkawy, Aya Abdulnasser Saed Ataya, Dohyeon Yeo, Eunsol An, Seokhyun Hwang, and SeungJun Kim. 2024. SYNC-VR: Synchronizing Your Senses to Conquer Motion Sickness for Enriching In-Vehicle Virtual Reality. In *Proceedings of the CHI Conference on Human Factors in Computing Systems*. 1–17.

[23] Marco Ewerton, Oleg Arenz, and Jan Peters. 2020. Assisted teleoperation in changing environments with a mixture of virtual guides. *Advanced Robotics* 34, 18 (2020), 1157–1170.

[24] Martha Flanders. 1991. Temporal patterns of muscle activation for arm movements in three-dimensional space. *Journal of Neuroscience* 11, 9 (1991), 2680–2693.

[25] MARTHA Flanders and JOHN F Soechting. 1990. Arm muscle activation for static forces in three-dimensional space. *Journal of Neurophysiology* 64, 6 (1990), 1818–1837.

[26] Péter Galambos. 2012. Vibrotactile feedback for haptics and telemanipulation: Survey, concept and experiment. *Acta Polytechnica Hungarica* 9, 1 (2012), 41–65.

[27] Geomagic. 2012. Phantom Omni ® haptic devices. retrieved February 29, 2013 from https://www.3dsystems.com/haptics-devices/touch.

[28] Geomagic. 2012. Phantom Premium ® haptic devices. retrieved February 29, 2013 from https://www.3dsystems.com/haptics-devices/3d-systems-phantom-premium.

[29] Claudia González, J Ernesto Solanes, Adolfo Munoz, Luis Gracia, Vicent Girbés-Juan, and Josep Tornero. 2021. Advanced teleoperation and control system for industrial robots based on augmented virtuality and haptic feedback. *Journal of Manufacturing Systems* 59 (2021), 283–298.

[30] Matthew Green, Yoon No Gregory Hong, Jinsook Roh, and Benjamin J Fregly. 2022. Computational modeling and simulation of closed chain arm-robot multibody dynamic systems in OpenSim. *Multibody System Dynamics* 56, 4 (2022), 313–334.

[31] Yanbin Guo, Yingbin Liu, Wenxuan Sun, Shuai Yu, Xiao-Jian Han, Xin-Hui Qu, and Guoping Wang. 2023. Digital twin-driven dynamic monitoring system of the upper limb force. *Computer Methods in Biomechanics and Biomedical Engineering* (2023), 1–13.

[32] Akif Hacinecipoglu, E Ilhan Konukseven, and A Bugra Koku. 2013. Evaluation of haptic feedback cues on vehicle teleoperation performance in an obstacle avoidance scenario. In *2013 World Haptics Conference (WHC)*. IEEE, 689–694.

[33] David M Halliday and Simon F Farmer. 2010. On the need for rectification of surface EMG. *Journal of neurophysiology* 103, 6 (2010), 3547–3547.

[34] Bingjian Huang, Zhecheng Wang, Qilong Cheng, Siyi Ren, Hanfeng Cai, Antonio Alvarez Valdivia, Karthik Mahadevan, and Daniel Wigdor. 2024. AeroHaptix: A Wearable Vibrotactile Feedback System for Enhancing Collision Avoidance in UAV Teleoperation. *arXiv preprint arXiv:2407.12105* (2024).

[35] Seokhyun Hwang, Seongjun Kang, Jeongseok Oh, Jeongju Park, Semoo Shin, Yiyue Luo, Joseph DelPreto, Wojciech Matusik, Daniela Rus, and SeungJun Kim. 2024. Proposal of a Framework for Enhancing Teleoperation Experience with Biomechanical Simulation-Based Electrical Muscle Stimulation in Virtual Reality. In *Companion of the 2024 on ACM International Joint Conference on Pervasive and Ubiquitous Computing*. 826–831.

[36] Seokhyun Hwang, YoungIn Kim, Youngseok Seo, and SeungJun Kim. 2023. Enhancing Seamless Walking in Virtual Reality: Application of Bone-Conduction Vibration in Redirected Walking. In *2023 IEEE International Symposium on Mixed and Augmented Reality (ISMAR)*. IEEE, 1181–1190.

[37] Seokhyun Hwang, Jieun Lee, YoungIn Kim, and SeungJun Kim. 2022. REVES: Redirection Enhancement Using Four-Pole Vestibular Electrode Stimulation. In *CHI Conference on Human Factors in Computing Systems Extended Abstracts*. 1–7.

[38] Seokhyun Hwang, Jieun Lee, Youngin Kim, Youngseok Seo, and Seungjun Kim. 2023. Electrical, Vibrational, and Cooling Stimuli-Based Redirected Walking:

Comparison of Various Vestibular Stimulation-Based Redirected Walking Systems. In *Proceedings of the 2023 CHI Conference on Human Factors in Computing Systems*. 1–18.
[39] Seokhyun Hwang, Jeongseok Oh, Seongjun Kang, Minwoo Seong, Ahmed Ibrahim Ahmed Mohamed Elsharkawy, and SeungJun Kim. 2024. Ergopulse: Electrifying your lower body with biomechanical simulation-based electrical muscle stimulation haptic system in virtual reality. In *Proceedings of the CHI Conference on Human Factors in Computing Systems*. 1–21.
[40] Novint Technologies Inc. 2013. Novint Falcon haptic device. retrieved February 29, 2013 from http://www.novint.com/.
[41] Akira Ito, Yasunori Yamamoto, Masanori Sato, Kazushi Ikeda, Masahiro Yamamoto, Hideaki Fujita, Eiji Nagamori, Yoshinori Kawabe, and Masamichi Kamihira. 2014. Induction of functional tissue-engineered skeletal muscle constructs by defined electrical stimulation. *Scientific reports* 4, 1 (2014), 4781.
[42] Shubham Jain, Shubham Sharma, and Dhawal Babbar. 2017. Star-force: A playful implementation of the jedi-force. In *Proceedings of the Eleventh International Conference on Tangible, Embedded, and Embodied Interaction*. 761–766.
[43] Inseong Jo, Younkyu Park, and Joonbum Bae. 2013. A teleoperation system with an exoskeleton interface. In *2013 IEEE/ASME International Conference on Advanced Intelligent Mechatronics*. IEEE, 1649–1654.
[44] Taewoo Jo, Dohyeon Yeo, Gwangbin Kim, Seokhyun Hwang, and SeungJun Kim. 2024. WatchCap: Improving Scanning Efficiency in People with Low Vision through Compensatory Head Movement Stimulation. *Proceedings of the ACM on Interactive, Mobile, Wearable and Ubiquitous Technologies* 8, 2 (2024), 1–32.
[45] Tero Kaarlela, Tomi Pitkäaho, Sakari Pieskä, Paulo Padrão, Leonardo Bobadilla, Matti Tikanmäki, Timo Haavisto, Víctor Blanco Bataller, Niko Laivuori, and Mika Luimula. 2023. Towards metaverse: Utilizing extended reality and digital twins to control robotic systems. In *Actuators*, Vol. 12. MDPI, 219.
[46] Seongjun Kang, Gwangbin Kim, Seokhyun Hwang, Jeongju Park, Ahmed Elsharkawy, and SeungJun Kim. 2024. Dual-sided Peltier Elements for Rapid Thermal Feedback in Wearables. *arXiv preprint arXiv:2405.11807* (2024).
[47] Seongjun Kang, Gwangbin Kim, Seokhyun Hwang, Jeongju Park, Ahmed Ibrahim Ahmed Mohamed Elsharkawy, and SeungJun Kim. 2024. Flip-Pelt: Motor-Driven Peltier Elements for Rapid Thermal Stimulation and Congruent Pressure Feedback in Virtual Reality. In *Proceedings of the 37th Annual ACM Symposium on User Interface Software and Technology*. 1–15.
[48] Seongjun Kang, Gwangbin Kim, and SeungJun Kim. 2023. Giant Finger: A Novel Visuo-Somatosensory Approach to Simulating Lower Body Movements in Virtual Reality. In *2023 IEEE International Symposium on Mixed and Augmented Reality (ISMAR)*. IEEE, 233–242.
[49] Seongjun Kang, Gwangbin Kim, Kyung-Taek Lee, and SeungJun Kim. 2023. Giant Finger: Visuo-proprioceptive congruent virtual legs for flying actions in virtual reality. In *2023 IEEE Conference on Virtual Reality and 3D User Interfaces Abstracts and Workshops (VRW)*. IEEE, 933–934.
[50] Shunichi Kasahara, Jun Nishida, and Pedro Lopes. 2019. Preemptive action: Accelerating human reaction using electrical muscle stimulation without compromising agency. In *Proceedings of the 2019 CHI Conference on Human Factors in Computing Systems*. 1–15.
[51] Jinwook Kim, Seonghyeon Kim, and Jeongmi Lee. 2022. The effect of multisensory pseudo-haptic feedback on perception of virtual weight. *IEEE Access* 10 (2022), 5129–5140.
[52] YoungIn Kim, Seokhyun Hwang, Jeongseok Oh, and Seungjun Kim. 2024. GaitWay: Gait Data-Based VR Locomotion Prediction System Robust to Visual Distraction. In *Extended Abstracts of the CHI Conference on Human Factors in Computing Systems*. 1–8.
[53] Rex B Kline. 2023. *Principles and practice of structural equation modeling*. Guilford publications.
[54] Michinari Kono, Takashi Miyaki, and Jun Rekimoto. 2018. In-pulse: inducing fear and pain in virtual experiences. In *Proceedings of the 24th ACM Symposium on Virtual Reality Software and Technology*. 1–5.
[55] Katherine J Kuchenbecker, Jonathan Fiene, and Günter Niemeyer. 2006. Improving contact realism through event-based haptic feedback. *IEEE transactions on visualization and computer graphics* 12, 2 (2006), 219–230.
[56] Yosuke Kurihara, Taku Hachisu, Katherine J Kuchenbecker, and Hiroyuki Kajimoto. 2013. Jointonation: robotization of the human body by vibrotactile feedback. In *SIGGRAPH Asia 2013 Emerging Technologies*. 1–3.
[57] Yuichi Kurita, Takaaki Ishikawa, and Toshio Tsuji. 2016. Stiffness display by muscle contraction via electric muscle stimulation. *IEEE Robotics and Automation Letters* 1, 2 (2016), 1014–1019.
[58] Melissa J Lambeth and Martin J Kushmerick. 2002. A computational model for glycogenolysis in skeletal muscle. *Annals of biomedical engineering* 30 (2002), 808–827.
[59] Corinna E Lathan and Michael Tracey. 2002. The effects of operator spatial perception and sensory feedback on human-robot teleoperation performance. *Presence* 11, 4 (2002), 368–377.
[60] Chang Kee Lee, Chang Gyu Lee, Jungmin Yun, Ohung Kwon, and Dae Young Lim. 2023. Biocompatible Electric Muscle Stimulation Pads with Enhanced Skin Adhesion for Stable Signal Transmission During Varied Physical Movements. In *International Conference on Human-Computer Interaction*. Springer, 49–54.
[61] Jieun Lee, Seokhyun Hwang, Aya Ataya, and SeungJun Kim. 2024. Effect of optical flow and user VR familiarity on curvature gain thresholds for redirected walking. *Virtual Reality* 28, 1 (2024), 35.
[62] Jieun Lee, Seokhyun Hwang, Kyunghwan Kim, and SeungJun Kim. 2022. Auditory and olfactory stimuli-based attractors to induce reorientation in virtual reality forward redirected walking. In *CHI conference on human factors in computing systems extended abstracts*. 1–7.
[63] Jieun Lee, Seokhyun Hwang, Kyunghwan Kim, and SeungJun Kim. 2024. Evaluation of visual, auditory, and olfactory stimulus-based attractors for intermittent reorientation in virtual reality locomotion. *Virtual Reality* 28, 2 (2024), 104.
[64] Jungeun Lee, Yeongjin Kim, and Hoeryong Jung. 2020. Electrically Elicited Force Response Characteristics of Forearm Extensor Muscles for Electrical Muscle Stimulation-Based Haptic Rendering. *Sensors* 20, 19 (2020), 5669.
[65] M Levy, J Mizrahi, and Z Susak. 1990. Recruitment, force and fatigue characteristics of quadriceps muscles of paraplegics isometrically activated by surface functional electrical stimulation. *Journal of biomedical engineering* 12, 2 (1990), 150–156.
[66] Jing Z Liu, Robert W Brown, and Guang H Yue. 2002. A dynamical model of muscle activation, fatigue, and recovery. *Biophysical journal* 82, 5 (2002), 2344–2359.
[67] Pedro Lopes and Patrick Baudisch. 2013. Muscle-propelled force feedback: bringing force feedback to mobile devices. In *Proceedings of the SIGCHI Conference on Human Factors in Computing Systems*. 2577–2580.
[68] Pedro Lopes, Alexandra Ion, and Patrick Baudisch. 2015. Impacto: Simulating physical impact by combining tactile stimulation with electrical muscle stimulation. In *Proceedings of the 28th annual ACM symposium on user interface software & technology*. 11–19.
[69] Pedro Lopes, Alexandra Ion, Willi Mueller, Daniel Hoffmann, Patrik Jonell, and Patrick Baudisch. 2015. Proprioceptive interaction. In *Proceedings of the 33rd annual acm conference on human factors in computing systems*. 939–948.
[70] Pedro Lopes, Sijing You, Lung-Pan Cheng, Sebastian Marwecki, and Patrick Baudisch. 2017. Providing haptics to walls & heavy objects in virtual reality by means of electrical muscle stimulation. In *Proceedings of the 2017 CHI Conference on Human Factors in Computing Systems*. 1471–1482.
[71] Pedro Lopes, Sijing You, Alexandra Ion, and Patrick Baudisch. 2018. Adding force feedback to mixed reality experiences and games using electrical muscle stimulation. In *Proceedings of the 2018 chi conference on human factors in computing systems*. 1–13.
[72] Pedro Lopes, Sijing Young, Lung-pan Cheng, P Marwecki, and Patrick Baudisch. [n. d.]. Providing haptics to walls and other heavy objects in virtual reality by means of electrical muscle stimulation. In *Proc. Conf. Human Factors in Computing Systems*.
[73] Daniel C McFarland, Emily M McCain, Michael N Poppo, and Katherine R Saul. 2019. Spatial dependency of glenohumeral joint stability during dynamic unimanual and bimanual pushing and pulling. *Journal of biomechanical engineering* 141, 5 (2019), 051006.
[74] M Alejandra Menchaca-Brandan, Andrew M Liu, Charles M Oman, and Alan Natapoff. 2007. Influence of perspective-taking and mental rotation abilities in space teleoperation. In *Proceedings of the ACM/IEEE International Conference on Human-robot interaction*. 271–278.
[75] Inc. Meta Platforms. 2024. Movement SDK for Unity. https://github.com/oculus-samples/Unity-Movement. Accessed: 2024-09-12.
[76] Matthew Millard, Thomas Uchida, Ajay Seth, and Scott L Delp. 2013. Flexing computational muscle: modeling and simulation of musculotendon dynamics. *Journal of biomechanical engineering* 135, 2 (2013), 021005.
[77] Robin R Murphy, Karen L Dreger, Sean Newsome, Jesse Rodocker, Eric Steimle, Tetsuya Kimura, Kenichi Makabe, Fumitoshi Matsuno, Satoshi Tadokoro, and Kazuyuki Kon. 2011. Use of remotely operated marine vehicles at Minamisanriku and Rikuzentakata Japan for disaster recovery. In *2011 IEEE International symposium on safety, security, and rescue robotics*. IEEE, 19–25.
[78] LJ Myers, M Lowery, M O'malley, CL Vaughan, C Heneghan, A St Clair Gibson, YXR Harley, and R Sreenivasan. 2003. Rectification and non-linear preprocessing of EMG signals for cortico-muscular analysis. *Journal of neuroscience methods* 124, 2 (2003), 157–165.
[79] Arinobu Niijima, Toki Takeda, Ryosuke Aoki, and Shinji Miyahara. 2022. Muscle synergies learning with electrical muscle stimulation for playing the piano. In *Proceedings of the 35th Annual ACM Symposium on User Interface Software and Technology*. 1–10.
[80] Niels Christian Nilsson, Stefania Serafin, and Rolf Nordahl. 2016. Walking in place through virtual worlds. In *International Conference on Human-Computer Interaction*. Springer, 37–48.
[81] Verena Nitsch and Berthold Färber. 2012. A meta-analysis of the effects of haptic interfaces on task performance with teleoperation systems. *IEEE transactions on haptics* 6, 4 (2012), 387–398.
[82] Vahid Noei and Heba Lakany. 2022. Analysis of movement of an elbow joint with a wearable robotic exoskeleton Using OpenSim software. In *2022 44th Annual International Conference of the IEEE Engineering in Medicine & Biology*

Society (EMBC). IEEE, 4342–4345.

[83] Donald A Norman. 1986. User-centered System Design: New Perspectives on Human–computer Interaction.

[84] Shahin S Nudehi, Ranjan Mukherjee, and Moji Ghodoussi. 2003. A haptic interface design for minimally invasive telesurgical training and collaboration in the presence of time delay. In *42nd IEEE International Conference on Decision and Control (IEEE Cat. No. 03CH37475)*, Vol. 5. IEEE, 4563–4568.

[85] Allison M Okamura. 2004. Methods for haptic feedback in teleoperated robot-assisted surgery. *Industrial Robot: An International Journal* 31, 6 (2004), 499–508.

[86] Yoshiaki Omura. 1985. Electrical parameters for safe and effective electro-acupuncture and transcutaneous electrical stimulation: Threshold potentials for tingling, muscle contraction and pain; and how to prevent adverse effects of electro-therapy part i. *Acupuncture & electro-therapeutics research* 10, 4 (1985), 335–337.

[87] Claudio Pacchierotti, Domenico Prattichizzo, and Katherine J Kuchenbecker. 2015. Cutaneous feedback of fingertip deformation and vibration for palpation in robotic surgery. *IEEE Transactions on Biomedical Engineering* 63, 2 (2015), 278–287.

[88] Daniel Pamungkas and Koren Ward. 2015. Immersive teleoperation of a robot arm using electro-tactile feedback. In *2015 6th International Conference on Automation, Robotics and Applications (ICARA)*. IEEE, 300–305.

[89] Daniel S Pamungkas and Koren Ward. 2013. Tele-operation of a robot arm with electro tactile feedback. In *2013 IEEE/ASME International Conference on Advanced Intelligent Mechatronics*. IEEE, 704–709.

[90] FJ Perez-Grau, R Ragel, F Caballero, A Viguria, and A Ollero. 2017. Semi-autonomous teleoperation of UAVs in search and rescue scenarios. In *2017 International Conference on Unmanned Aircraft Systems (ICUAS)*. IEEE, 1066–1074.

[91] Max Pfeiffer, Tim Duente, and Michael Rohs. 2016. Let your body move: a prototyping toolkit for wearable force feedback with electrical muscle stimulation. In *Proceedings of the 18th International Conference on Human-Computer Interaction with Mobile Devices and Services*. 418–427.

[92] Max Pfeiffer and Michael Rohs. 2017. Haptic feedback for wearables and textiles based on electrical muscle stimulation. *Smart Textiles: Fundamentals, Design, and Interaction* (2017), 103–137.

[93] Michael O Powell, Aviv Elor, Ash Robbins, Sri Kurniawan, and Mircea Teodorescu. 2022. Predictive shoulder kinematics of rehabilitation exercises through immersive virtual reality. *IEEE Access* 10 (2022), 25621–25632.

[94] M Ora Powell, Aviv Elor, Mircea Teodorescu, and Sri Kurniawan. 2020. Openbutterfly: Multimodal rehabilitation analysis of immersive virtual reality for physical therapy. *American Journal of Sports Science and Medicine* 8, 1 (2020), 23–35.

[95] Efi Psomopoulou, Raj Persad, Anthony Koupparis, Sajeeva Abeywardena, Mohammad Fattahi Sani, Chris Melhuish, and Sanja Dogramadzi. 2020. Evaluation of force feedback for palpation and application of active constraints on a teleoperated system. In *XV Mediterranean Conference on Medical and Biological Engineering and Computing–MEDICON 2019: Proceedings of MEDICON 2019, September 26-28, 2019, Coimbra, Portugal*. Springer, 1571–1580.

[96] M. Rathore, S. Trivedi, Jessy Abraham, and M. Sinha. 2017. Anatomical Correlation of Core Muscle Activation in Different Yogic Postures. *International Journal of Yoga* 10 (2017), 59 – 66. https://doi.org/10.4103/0973-6131.205515

[97] Sharif Razzaque, Zachariah Kohn, and Mary C. Whitton. 2001. Redirected Walking. In *Eurographics 2001 - Short Presentations*. Eurographics Association. https://doi.org/10.2312/egs.20011036

[98] A Reiter, V Nitsch, G Reinhart, and B Färber. 2009. Effects of visual and haptic feedback on telepresent micro assembly tasks. In *3rd International Conference on Changeable, Agile, Reconfigurable and Virtual Production CARV*.

[99] Jinsook Roh, William Z Rymer, and Randall F Beer. 2012. Robustness of muscle synergies underlying three-dimensional force generation at the hand in healthy humans. *Journal of neurophysiology* 107, 8 (2012), 2123–2142.

[100] Joseph M Romano, Robert J Webster, and Allison M Okamura. 2007. Teleoperation of steerable needles. In *Proceedings 2007 IEEE International Conference on Robotics and Automation*. IEEE, 934–939.

[101] Azhar Aulia Saputra, Chin Wei Hong, Tadamitsu Matsuda, and Naoyuki Kubota. 2023. A real-time control system of upper-limb human musculoskeletal model with environmental integration. *IEEE access* (2023).

[102] Katherine R Saul, Xiao Hu, Craig M Goehler, Meghan E Vidt, Melissa Daly, Anca Velisar, and Wendy M Murray. 2015. Benchmarking of dynamic simulation predictions in two software platforms using an upper limb musculoskeletal model. *Computer methods in biomechanics and biomedical engineering* 18, 13 (2015), 1445–1458.

[103] Ambika Shahu, Khaled Kassem, Leonhard Zehetgruber, Philipp Wintersberger, and Florian Michahelles. 2023. Electrifying Obstacle Avoidance: Enhancing Teleoperation of Robots with EMS-Assisted Obstacle Avoidance. In *HHAI 2023: Augmenting Human Intellect*. IOS Press, 224–233.

[104] Thomas B Sheridan. 1993. Space teleoperation through time delay: Review and prognosis. *IEEE Transactions on robotics and Automation* 9, 5 (1993), 592–606.

[105] Mel Slater, Martin Usoh, and Anthony Steed. 1995. Taking steps: the influence of a walking technique on presence in virtual reality. *ACM Transactions on Computer-Human Interaction (TOCHI)* 2, 3 (1995), 201–219.

[106] Akifumi Takahashi, Yudai Tanaka, Archit Tamhane, Alan Shen, Shan-Yuan Teng, and Pedro Lopes. 2024. Can a Smartwatch Move Your Fingers? Compact and Practical Electrical Muscle Stimulation in a Smartwatch. In *Proceedings of the 37th Annual ACM Symposium on User Interface Software and Technology*. 1–15.

[107] Yudai Tanaka, Akifumi Takahashi, and Pedro Lopes. 2023. Interactive Benefits from Switching Electrical to Magnetic Muscle Stimulation. In *Proceedings of the 36th Annual ACM Symposium on User Interface Software and Technology*. 1–12.

[108] Russell H Taylor, Arianna Menciassi, Gabor Fichtinger, Paolo Fiorini, and Paolo Dario. 2016. Medical robotics and computer-integrated surgery. *Springer handbook of robotics* (2016), 1657–1684.

[109] Daria Trinitatova and Dzmitry Tsetserukou. 2023. Study of the Effectiveness of a Wearable Haptic Interface With Cutaneous and Vibrotactile Feedback for VR-Based Teleoperation. *IEEE Transactions on Haptics* 16, 4 (2023), 463–469.

[110] Marc Ueberle, Nico Mock, and Martin Buss. 2004. Vishard10, a novel hyper-redundant haptic interface. In *12th International Symposium on Haptic Interfaces for Virtual Environment and Teleoperator Systems, 2004. HAPTICS'04. Proceedings*. IEEE, 58–65.

[111] Juwon Um, Eunki Jeon, Yumin Kang, Seongjun Kang, Ahmed Elsharkawy, Joseph DelPreto, Wojciech Matusik, Daniela Rus, and SeungJun Kim. 2024. LegSense: Inducing Walking Sensation in Seated VR by Providing Movement Illusion via Electrical Muscle Stimulation. In *Companion of the 2024 on ACM International Joint Conference on Pervasive and Ubiquitous Computing*. 797–802.

[112] Myla van Wegen, Just L Herder, Rolf Adelsberger, Manuela Pastore-Wapp, Erwin EH Van Wegen, Stephan Bohlhalter, Tobias Nef, Paul Krack, and Tim Vanbellingen. 2023. An overview of wearable haptic technologies and their performance in virtual object exploration. *Sensors* 23, 3 (2023), 1563.

[113] Michael E Walker, Hooman Hedayati, and Daniel Szafir. 2019. Robot teleoperation with augmented reality virtual surrogates. In *2019 14th ACM/IEEE International Conference on Human-Robot Interaction (HRI)*. IEEE, 202–210.

[114] Bernhard Weber and Clara Eichberger. 2015. The benefits of haptic feedback in telesurgery and other teleoperation systems: a meta-analysis. In *Universal Access in Human-Computer Interaction. Access to Learning, Health and Well-Being: 9th International Conference, UAHCI 2015, Held as Part of HCI International 2015, Los Angeles, CA, USA, August 2-7, 2015, Proceedings, Part III 9*. Springer, 394–405.

[115] Anthony S Wexler, Jun Ding, and Stuart A Binder-Macleod. 1997. A mathematical model that predicts skeletal muscle force. *IEEE transactions on biomedical engineering* 44, 5 (1997), 337–348.

[116] Bob G Witmer and Michael J Singer. 1998. Measuring presence in virtual environments: A presence questionnaire. *Presence* 7, 3 (1998), 225–240.

[117] RD Woittiez, PA Huijing, HBK Boom, and RH Rozendal. 1984. A three-dimensional muscle model: a quantified relation between form and function of skeletal muscles. *Journal of Morphology* 182, 1 (1984), 95–113.

[118] JH Won, Gi-Hun Yang, and Jae Wook Jeon. 2015. A novel wireless vibrotactile display device for representing 3DOF force feedback in teleoperation. In *2015 IEEE International Conference on Advanced Intelligent Mechatronics (AIM)*. IEEE, 1749–1753.

[119] F. Wörgötter, Bailu Si, L. Ting, M. H. Sohn, M. Hongchul Sohn, G. Woodruff, and Ting Sohn. 2016. Suboptimal Muscle Synergy Activation Patterns Generalize their Motor Function across Postures. *Frontiers in Computational Neuroscience* 10 (2016). https://doi.org/10.3389/fncom.2016.00007

[120] Pengxiang Xia, Fang Xu, Zhuoyuan Song, Shuai Li, and Jing Du. 2023. Sensory augmentation for subsea robot teleoperation. *Computers in Industry* 145 (2023), 103836.

[121] David A Ziegler, Jacqueline R Janowich, and Adam Gazzaley. 2018. Differential impact of interference on internally-and externally-directed attention. *Scientific reports* 8, 1 (2018), 2498.

A Significance Test Results

Table 2: Statistics and significance test results from E1

Statistics		**Significance**	**Statistics**		**Significance**
Biceps			**Triceps**		
TelePulse	$M = .387$, $SE = .140$	$t(7) = -3.518$	TelePulse	$M = .333$, $SE = .144$	$t(7) = -3.911$
NonBioSim	$M = .858$, $SE = .012$	$p = .010^{*}$	Baseline	$M = .936$, $SE = .031$	$p = .006^{**}$
ECRL			**ECU**		
TelePulse	$M = .291$, $SE = .092$	$t(7) = -5.485$	TelePulse	$M = .214$, $SE = .028$	$t(7) = -13.759$
NonBioSim	$M = .836$, $SE = .140$	$p < .001^{***}$	NonBioSim	$M = .829$, $SE = .025$	$p < .001^{***}$
FCR			**FCU**		
TelePulse	$M = .380$, $SE = .097$	$t(7) = -4.438$	TelePulse	$M = .237$, $SE = .061$	$t(7) = -8.475$
NonBioSim	$M = .895$, $SE = .031$	$p = .003^{**}$	NonBioSim	$M = .891$, $SE = .029$	$p < .001^{***}$
Overall					
TelePulse	$M = .307$, $SE = .032$	$t(7) = -16.110$			
NonBioSim	$M = .873$, $SE = .021$	$p < .001^{***}$			
Left			**Right**		
TelePulse	$M = .329$, $SE = .044$	$t(7) = -9.350$	TelePulse	$M = .331$, $SE = .023$	$t(7) = -14.763$
NonBioSim	$M = .872$, $SE = .018$	$p < .001^{***}$	NonBioSim	$M = .842$, $SE = .029$	$p < .001^{***}$
Up			**Down**		
TelePulse	$M = .306$, $SE = .048$	$t(7) = -11.237$	TelePulse	$M = .257$, $SE = .050$	$t(7) = -12.255$
NonBioSim	$M = .858$, $SE = .017$	$p < .001^{***}$	NonBioSim	$M = .881$, $SE = .025$	$p < .001^{***}$
Forward			**Backward**		
TelePulse	$M = .339$, $SE = .042$	$t(7) = -11.104$	TelePulse	$M = .280$, $SE = .031$	$t(7) = -24.285$
NonBioSim	$M = .907$, $SE = .048$	$p < .001^{***}$	NonBioSim	$M = .886$, $SE = .019$	$p < .001^{***}$
Overall					
TelePulse	$M = .317$, $SE = .011$	$t(7) = -37.727$			
NonBioSim	$M = .874$, $SE = .014$	$p < .001^{***}$			

Table 3: Significance test results of E2 sanding task

RM ANOVA	**Post-hoc test**			
Mean Absolute Error				
$F(3, 21) = 5.257$	Baseline-NonBioSim	$p = 1.000$	Baseline-TelePulse	$p = .012^{*}$
$p = .007^{**}$	Baseline-ElecTac	$p = 1.000$	NonBioSim-TelePulse	$p = .021^{*}$
	NonBioSim-ElecTac	$p = 1.000$	TelePulse-ElecTac	$p = .043^{*}$
PQ - Total				
$F(3, 21) = 6.110$	Baseline-NonBioSim	$p = .399$	Baseline-TelePulse	$p = .004^{**}$
$p = .004^{**}$	Baseline-ElecTac	$p = .115$	NonBioSim-TelePulse	$p = .033^{*}$
	NonBioSim-ElecTac	$p = .399$	TelePulse-ElecTac	$p = .315$
PQ - Control				
$F(3, 21) = 3.799$	Baseline-NonBioSim	$p = .704$	Baseline-TelePulse	$p = .162$
$p = .025^{*}$	Baseline-ElecTac	$p = .704$	NonBioSim-TelePulse	$p = .023^{*}$
	NonBioSim-ElecTac	$p = .324$	TelePulse-ElecTac	$p = .520$
PQ - Sensory				
$F(3, 21) = 13.480$	Baseline-NonBioSim	$p = .002^{**}$	Baseline-TelePulse	$p < .001^{***}$
$p < .001^{***}$	Baseline-ElecTac	$p < .001^{***}$	NonBioSim-TelePulse	$p = .246$
	NonBioSim-ElecTac	$p = .629$	TelePulse-ElecTac	$p = .392$
PQ - Distraction				
$F(3, 21) = 3.966$	Baseline-NonBioSim	$p = .064$	Baseline-TelePulse	$p = .037^{*}$
$p = .022^{*}$	Baseline-ElecTac	$p = .065$	NonBioSim-TelePulse	$p = 1.000$
	NonBioSim-ElecTac	$p = 1.000$	TelePulse-ElecTac	$p = 1.000$
PQ - Realism				
$F(3, 21) = 9.508$	Baseline-NonBioSim	$p = .188$	Baseline-TelePulse	$p < .001^{***}$
$p < .001^{***}$	Baseline-ElecTac	$p = .031^{*}$	NonBioSim-TelePulse	$p = .012^{*}$
	NonBioSim-ElecTac	$p = .248$	TelePulse-ElecTac	$p = .107$

Table 4: Significance test results of E2 drilling task.

RM ANOVA	Post-hoc test			
PQ - Total				
$F(3, 21) = 14.321$	Baseline-NonBioSim	$p = .006^{**}$	Baseline-TelePulse	$p < .001^{**}$
$p < .001^{***}$	Baseline-ElecTac	$p = .070$	NonBioSim-TelePulse	$p = .039^{*}$
	NonBioSim-ElacTac	$p = .169$	TelePulse-ElecTac	$p = .002^{**}$
PQ - Control				
$F(3, 21) = 6.964$	Baseline-NonBioSim	$p = .873$	Baseline-TelePulse	$p = .002^{**}$
$p = .002^{**}$	Baseline-ElecTac	$p = 1.000$	NonBioSim-TelePulse	$p = .021^{*}$
	NonBioSim-ElacTac	$p = 1.000$	TelePulse-ElecTac	$p = .009^{**}$
PQ - Sensory				
$F(3, 21) = 16.878$	Baseline-NonBioSim	$p = .002^{**}$	Baseline-TelePulse	$p < .001^{***}$
$p < .001^{***}$	Baseline-ElecTac	$p = .017^{*}$	NonBioSim-TelePulse	$p = .028^{*}$
	NonBioSim-ElacTac	$p = .228$	TelePulse-ElecTac	$p = .003^{**}$
PQ - Distraction				
$F(3, 21) = 2.506$	Baseline-NonBioSim	$p = .119$	Baseline-TelePulse	$p = 1.000$
$p = .087$	Baseline-ElecTac	$p = 1.000$	NonBioSim-TelePulse	$p = .212$
	NonBioSim-ElacTac	$p = .345$	TelePulse-ElecTac	$p = 1.000$
PQ - Realism				
$F(3, 21) = 13.313$	Baseline-NonBioSim	$p = .011^{*}$	Baseline-TelePulse	$p < .001^{***}$
$p < .001^{***}$	Baseline-ElecTac	$p = .100$	NonBioSim-TelePulse	$p = .034^{*}$
	NonBioSim-ElacTac	$p = .204$	TelePulse-ElecTac	$p = .003^{**}$

B Witmer-Singer Presence Questionnaire [116]

(1) How much were you able to control events?

NOT AT ALL SOMEWHAT COMPLETELY

☐ 1 ☐ 2 ☐ 3 ☐ 4 ☐ 5 ☐ 6 ☐ 7

(2) How responsive was the environment to actions that you initiated (or performed)?

NOT RESPONSIVE MODERATELY RESPONSIVE COMPLETELY RESPONSIVE

☐ 1 ☐ 2 ☐ 3 ☐ 4 ☐ 5 ☐ 6 ☐ 7

(3) How natural did your interactions with the environment seem?

EXTREMELY ARTIFICIAL BORDERLINE COMPLETELY NATURAL

☐ 1 ☐ 2 ☐ 3 ☐ 4 ☐ 5 ☐ 6 ☐ 7

(4) How completely were all of your senses engaged?

NOT ENGAGED MODERATELY ENGAGED COMPLETELY ENGAGED

☐ 1 ☐ 2 ☐ 3 ☐ 4 ☐ 5 ☐ 6 ☐ 7

(5) How much did the visual aspects of the environment involve you?

NOT AT ALL SOMEWHAT COMPLETELY

☐ 1 ☐ 2 ☐ 3 ☐ 4 ☐ 5 ☐ 6 ☐ 7

(6) How much did the auditory aspects of the environment involve you?

NOT AT ALL SOMEWHAT COMPLETELY

☐ 1 ☐ 2 ☐ 3 ☐ 4 ☐ 5 ☐ 6 ☐ 7

(7) How natural was the mechanism which controlled movement through the environment?

EXTREMELY ARTIFICIAL BORDERLINE COMPLETELY NATURAL

☐ 1 ☐ 2 ☐ 3 ☐ 4 ☐ 5 ☐ 6 ☐ 7

(8) How aware were you of events occurring in the real world around you?

NOT AWARE AT ALL MILDLY AWARE VERY AWARE

☐ 1 ☐ 2 ☐ 3 ☐ 4 ☐ 5 ☐ 6 ☐ 7

(9) How aware were you of your display and control devices?

NOT AWARE AT ALL MILDLY AWARE VERY AWARE

☐ 1 ☐ 2 ☐ 3 ☐ 4 ☐ 5 ☐ 6 ☐ 7

(10) How compelling was your sense of objects moving through space?

NOT AT ALL SOMEWHAT COMPLETELY

☐ 1 ☐ 2 ☐ 3 ☐ 4 ☐ 5 ☐ 6 ☐ 7

(11) How inconsistent or disconnected was the information coming from your various senses?

NOT AT ALL INCONSISTENT SOMEWHAT INCONSISTENT VERY INCONSISTENT

☐ 1 ☐ 2 ☐ 3 ☐ 4 ☐ 5 ☐ 6 ☐ 7

(12) How much did your experiences in the virtual environment seem consistent with your real-world experiences?

NOT CONSISTENT MODERATELY CONSISTENT VERY CONSISTENT

☐ 1 ☐ 2 ☐ 3 ☐ 4 ☐ 5 ☐ 6 ☐ 7

(13) Were you able to anticipate what would happen next in response to the actions that you performed?

NOT AT ALL SOMEWHAT COMPLETELY

☐ 1 ☐ 2 ☐ 3 ☐ 4 ☐ 5 ☐ 6 ☐ 7

(14) How completely were you able to actively survey or search the environment using vision?

NOT AT ALL SOMEWHAT COMPLETELY

☐ 1 ☐ 2 ☐ 3 ☐ 4 ☐ 5 ☐ 6 ☐ 7

(15) How well could you identify sounds?

NOT AT ALL SOMEWHAT COMPLETELY

☐ 1 ☐ 2 ☐ 3 ☐ 4 ☐ 5 ☐ 6 ☐ 7

(16) How well could you localize sounds?

NOT AT ALL SOMEWHAT COMPLETELY

☐ 1 ☐ 2 ☐ 3 ☐ 4 ☐ 5 ☐ 6 ☐ 7

(17) How well could you actively survey or search the virtual environment using touch?

NOT AT ALL SOMEWHAT COMPLETELY

☐ 1 ☐ 2 ☐ 3 ☐ 4 ☐ 5 ☐ 6 ☐ 7

(18) How compelling was your sense of moving around inside the virtual environment?

NOT COMPELLING MODERATELY COMPELLING VERY COMPELLING

☐ 1 ☐ 2 ☐ 3 ☐ 4 ☐ 5 ☐ 6 ☐ 7

(19) How closely were you able to examine objects?

NOT AT ALL | PRETTY CLOSELY | VERY CLOSELY

☐ 1 ☐ 2 ☐ 3 ☐ 4 ☐ 5 ☐ 6 ☐ 7

(20) How well could you examine objects from multiple viewpoints?

NOT AT ALL | SOMEWHAT | EXTENSIVELY

☐ 1 ☐ 2 ☐ 3 ☐ 4 ☐ 5 ☐ 6 ☐ 7

(21) How well could you move or manipulate objects in the virtual environment?

NOT AT ALL | SOMEWHAT | EXTENSIVELY

☐ 1 ☐ 2 ☐ 3 ☐ 4 ☐ 5 ☐ 6 ☐ 7

(22) To what degree did you feel confused or disoriented at the beginning of breaks or at the end of the experimental session?

NOT AT ALL | MILDLY DISORIENTED | VERY DISORIENTED

☐ 1 ☐ 2 ☐ 3 ☐ 4 ☐ 5 ☐ 6 ☐ 7

(23) How involved were you in the virtual environment experience?

NOT INVOLVED | MILDLY INVOLVED | COMPLETELY ENGROSSED

☐ 1 ☐ 2 ☐ 3 ☐ 4 ☐ 5 ☐ 6 ☐ 7

(24) How distracting was the control mechanism?

NOT AT ALL | MILDLY DISTRACTING | VERY DISTRACTING

☐ 1 ☐ 2 ☐ 3 ☐ 4 ☐ 5 ☐ 6 ☐ 7

(25) How much delay did you experience between your actions and expected outcomes?

NO DELAYS | MODERATE DELAYS | LONG DELAYS

☐ 1 ☐ 2 ☐ 3 ☐ 4 ☐ 5 ☐ 6 ☐ 7

(26) How quickly did you adjust to the virtual environment experience?

NOT AT ALL | SLOWLY | LESS THAN ONE MINUTE

☐ 1 ☐ 2 ☐ 3 ☐ 4 ☐ 5 ☐ 6 ☐ 7

(27) How proficient in moving and interacting with the virtual environment did you feel at the end of the experience?

NOT PROFICIENT | REASONABLY PROFICIENT | VERY PROFICIENT

☐ 1 ☐ 2 ☐ 3 ☐ 4 ☐ 5 ☐ 6 ☐ 7

(28) How much did the visual display quality interfere or distract you from performing assigned tasks or required activities?

NOT AT ALL | INTERFERED SOMEWHAT | PREVENTED PERFORMANCE

☐ 1 ☐ 2 ☐ 3 ☐ 4 ☐ 5 ☐ 6 ☐ 7

(29) How much did the control devices interfere with the performance of assigned tasks or with other activities?

NOT AT ALL | INTERFERED SOMEWHAT | INTERFERED GREATLY

☐ 1 ☐ 2 ☐ 3 ☐ 4 ☐ 5 ☐ 6 ☐ 7

(30) How well could you concentrate on the assigned tasks or required activities rather than on the mechanisms used to perform those tasks or activities?

NOT AT ALL | SOMEWHAT | COMPLETELY

☐ 1 ☐ 2 ☐ 3 ☐ 4 ☐ 5 ☐ 6 ☐ 7

(31) Did you learn new techniques that enabled you to improve your performance?

NO TECHNIQUES LEARNED | LEARNED SOME TECHNIQUES | LEARNED MANY TECHNIQUES

☐ 1 ☐ 2 ☐ 3 ☐ 4 ☐ 5 ☐ 6 ☐ 7

(32) Were you involved in the experimental task to the extent that you lost track of time?

NOT AT ALL | SOMEWHAT | COMPLETELY

☐ 1 ☐ 2 ☐ 3 ☐ 4 ☐ 5 ☐ 6 ☐ 7